STUDY OF CONTROLLERS FOR ENERGY MANAGEMENT IN ELECTRIC VEHICLES WITH ENERGY STORAGE(ESEV)

A Project Report

Submitted in partial fulfillment of requirements for
the award of the degree of

Bachelor and Master of Technology(Dual)

In

Electrical Engineering

By

K. Sai Manoj Reddy

(EE12B087)

Under the guidance of

Dr.K. S. Swarup

Department of Electrical Engineering

Indian Institute of Technology, Madras

March 2018

ABSTRACT

Electrical networks across the globe are gearing towards environmental friendly operation with many renewable sources being introduced. Renewable energy sources have attracted wide attention because of their abundant nature. They can be used for Energy Storage Electric Vehicle (ESEV) system.

The performance of a dual energy storage electric vehicle system mainly depends on the quality of its power and energy management. This project demonstrates the simulation of three different control strategies applied to an induction motor used in ESEV system. The DC output from PV boosted and it is applied to the Three Phase Inverter(TPI). The other DC input to the inverter is applied from a battery through a Bidirectional DC to DC Converter(BDDC). In forward mode, the power flows from battery to the induction motor of ESEV through BDDC and TPI. When the induction machine operates as a generator, the BDDC operates in reverse mode and the energy is pumped back to battery. The TPI converts DC into balanced three phase AC as needed by TPIM. The Simulink models for bidirectional ESEV in forward and reverse mode are developed and they are used for simulation studies. Simulation results of open loop ESEV system in forward and reverse modes are presented. Closed-loop PI,FOPID and FL-controlled Boost-converter based ESEV systems are designed, modeled, and simulated using Matlab Simulink and their results are conferred. Simulation studies are performed by considering change in input voltage and change in load torque of induction motor. The closed loop results are given in terms of time domain parameters like rise time, settling time and steady state error of speed. The explorations denote superior performance of FL-controlled ESEV system. The proposed closed loop ESEV has benefits like reduced error, bidirectional ability and fast dynamic response.

TABLE OF CONTENTS

LIST OF FIGURES

LIST OF TABLES

CHAPTER 1

INTRODUCTION

1.1 Introduction

The transportation sector is one of the major contributors to oil consumption. As a result, internal combustion engine vehicles like airplanes, cars, trucks, ships etc. are responsible for about 16% of the man-made CO2 all across the globe.

1.2 Literature Survey

In the United States, the transportation 1 sector is the second largest contributors of Green House Gases (GHG) [1], as it produces almost one-third of the emissions, which result in climate change [2]. It contributes to one 5th of the total CO2 emissions in the EU with this share constantly rising every year [3]. In order to combat climate change and global warming and to move towards a sustainable energy future, reducing emissions coming from transportation sector is quintessential. According to [4], EV can have a range of 40 miles on 8 kWh battery, emitting 0.26 pounds of CO2 per mile. Whereas a gasoline vehicle, with an economy of 30 mpg (miles per gallon), emits 0.6 pounds of CO2 per mile, and a 50-mpg emits around 0.4 pounds of CO2 per mile.

Therefore, a transition for electrification of the transportation sector is needed. In order to realize a transition to electric vehicles (EV), the customers need to be convinced to adopt this low carbon technology. Recent studies have been focused towards convenient charging solutions to EV customers [5, 6]. EVs form an integral part of the futuristic smart grid [7].

The increased adoption of EVs can prove to be a boon and bane both to the power grid in terms of the opportunities and challenges it will bring along. In [8], demonstrations have been made to show the negative impacts these newly added EVs would have on the power systems. In California, there are dedicated charging circuits for EV charging, and each charging circuit is equivalent to adding one house to the power grid. It can be looked upon as an additional burden because generally neighborhood circuits have only 5 to 10 houses [9].

Such occurrence shows us that, if there is a lack of coordination in the EV charging then, the large-scale deployment of EVs will cause issues in power system operation and scheduling [10]. To allow increased penetration of EVs without violation of system constraints, it is imperative to develop coordinated charging/ discharging scheduling algorithms for EVs [11].

EV charging co-ordination can be brought about in multiple ways if provisions are made available in the grid [12], [13], [14]. There can be several objectives for EV charging co-ordination including penetration maximization of EVs [12], and minimization of customer charging costs [13], [14]. Such EV coordination has been studied with Demand Response (DR) tools in [15], [16].

DR can be needed as the change in the usage of energy by customers in response to the variation in the electricity prices or to payments as incentives [17] by the retailer or the Utility Company. The objective of DR programs is two-fold: (i) minimizing electricity bills of the customers, and (ii) ensure the stability of the grid. Basically, there exist the following DR strategies, such 2 as 1) Price-based DR programs; 2) Incentive-based DR programs and 3) Demand reduction bids [18]. Demand response is an edacious way of demand control as it differs rates for electricity at different hours of the day.

Thus, with the help of this program, the customers can reduce their electricity expenses by shifting their price-elastic loads from peak hours. In price-based DR programs with the help of contractual arrangements between service providers and customers, the variation in electricity prices over time motivates the customers to alter the energy consumption [19]. It tries to in hence the customers such that they consume a reduced amount of energy when the wholesale electricity market prices shoot up or the power system reliability seems to be jeopardized [19]. Such DR programs are in proper coordination of EV [15]. Previously, several studies have been performed on DR programs in the smart grid [20{24].

In [20], the authors have worked on the scheduling problem for energy consumption, treating it to be a non-cooperative game between the consumers for strictly increasing cost functions, which are convex. In [21], the authors have taken into consideration a distributed system in which the dependency of the price on the overall load is utilized to model the price. Depending upon the price information, the users modify their electricity demand to maximize their utility. In [22], the authors have formulated a robust optimization problem such that the

utility of the user is maximized. [23] Maximizes energy efficiency and user satisfaction by exploiting the awareness of the users and also, suggested a way to manage and aggregate the preferences of the users.

In [24], they have proposed a scheme for dynamic pricing so as to attain an aggregated load prole, which will be suitable for the utilities. The DR problem has been studied for information sharing on different levels amongst the users in the smart grid. But the studies carried out in [20]- [24], either have a single source or some number of sources treated as a single entity, which make them limited in their scope. In [16], their study has included multiple consumers and UCs for maximizing their own payos, implementing the concept of Stackelberg game. With the substantial surge in the number of EVs and EV charging services, the potential of participating in DR programs by EV charging service providers has attracted considerable interest.

EV load is expected to cause an additional burden on the existing power grid but the fact that it is deferrable by nature makes it possible for the Utility Company (UC) to avail 3 adequate DR programs for EV customers. The EV customers can shift their load from peak to 0 peak period due to the elasticity of the EV load, resulting in the reduction of electricity costs, overall generation cost by attenuating the load curve, electricity market prices hence keeping the generation companies from the exertion of market power [25].

In this work, we are focusing on the price or rate based DR programs. In this type of DR program, electricity price varies over time such that the customers are motivated to shift their consumption and the implementation of DR is in accordance with the approved utility in deregulated markets. Studies in past have been focused on the design games for DR programs [16, 26{28]. Energy consumption games to 0, where an incentive to the users who cooperate, are formulated in [26] and [28].

However, the games are designed considering users as the only players. In [27], an optimal toU pricing method using game theory has been introduced without considering user constraints. Stackelberg games taking place between users and retailers were proposed in [16] and, [29], here the retailer declares its electricity price so as to maximize its revenue, as a response, every user then decides its consumption in accordance with it, to maximize its utility. However, the game in [16], [29] do not consider the EV load and hence the constraint imposed due to their charging

requirements. In [15], a demand response problem has been proposed as a game between a retailer and customers considering the constraints of EV charging at home. Though the Stackelberg game in [15] takes into consideration the EV load, it is limited in a way that there is only a single retailer which might not be the case in reality. Model indicating communication between multiple UCs and multiple customers is shown in Fig 1.1.

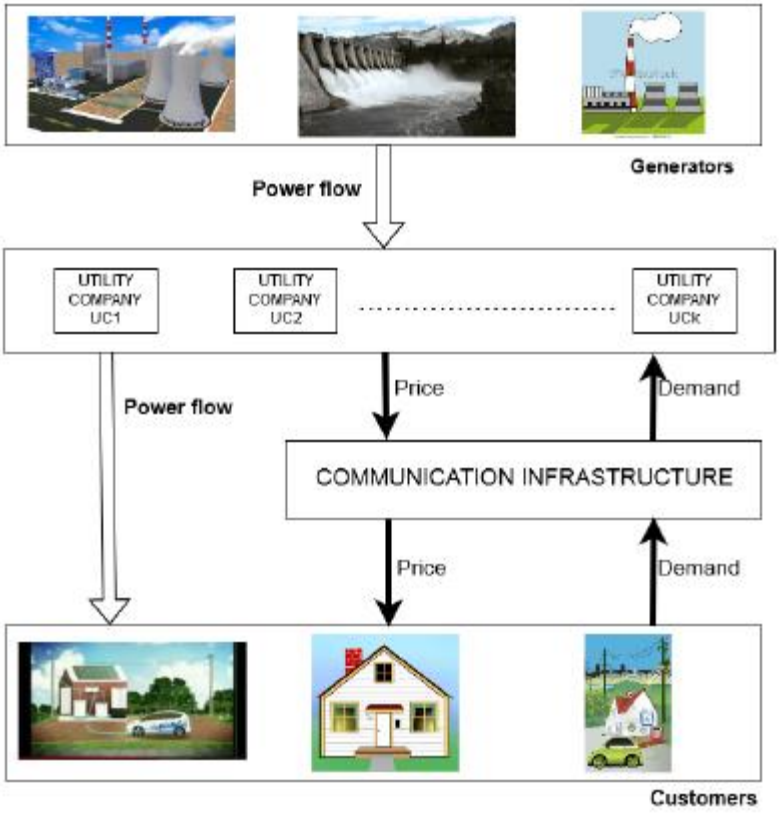

Fig. 1.1: Model-indicating communication between multiple UCs and multiple customers

The block diagram of energy storage vehicle system is shown in Figure 1.2.The two sources are battery and super capacitor.

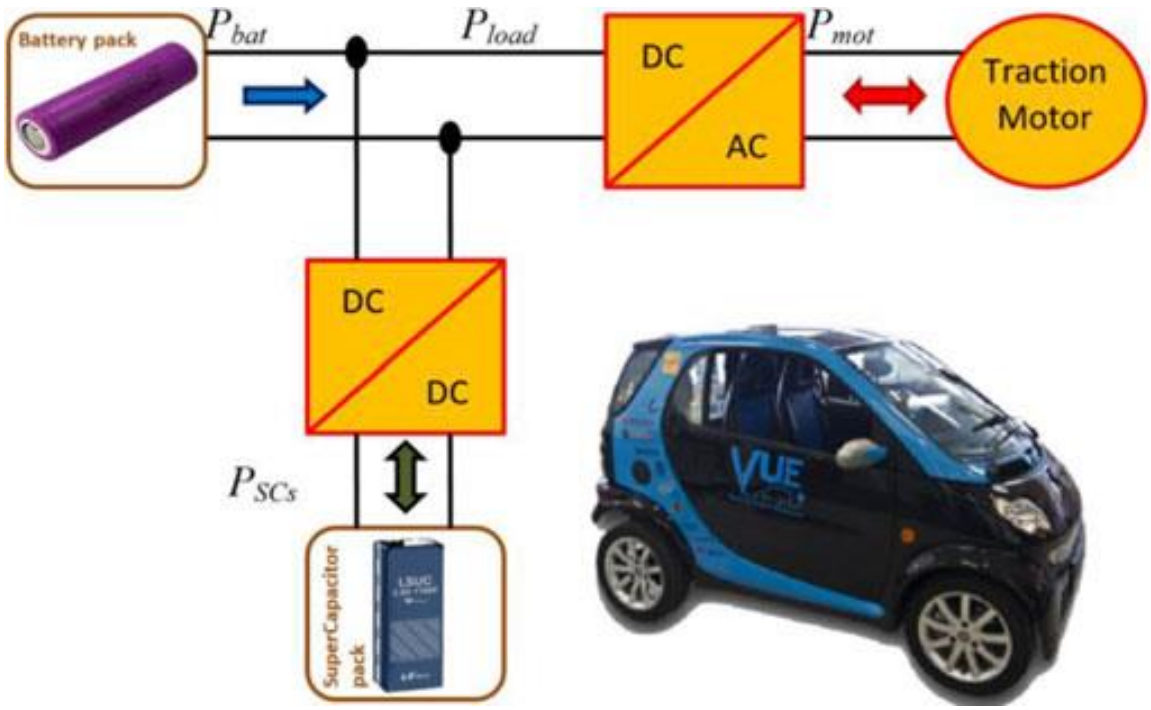

Fig.1.2 Block diagram of energy storage vehicle system

1.3 Research Gap

- The above papers do not deal with comparison of Responses of PI,FOPID and FL controlled ESEV systems.
- This work suggests FLC for the control of ESEV system.

1.4Objectives

- To transfer power in ESEV system in both the directions.
- To enhance dynamic response of the closed loop controlled ESEV system with an increase in load using a suitable controller.

1.5 Chapter Organization

- ***Chapter 1*** deals with introduction, literature survey, research gap, objectives, and block diagram of the proposed system.
- ***Chapter 2***depicts description of ESEV system.
- The simulation results of open loop ESEV system are presented in ***Chapter 3***.
- ***Chapter 4*** presents the closed loop simulation of ESEV system with the change in load torque.
- Closed loop simulation results of the ESEV system with the change in voltage are presented in ***Chapter 5***.
- The conclusion and contributions are given in *C**hapter 6.*** Scope for further work is also presented in this chapter.

1.6 Summary

Introduction, literature survey, research gap, objectives, and block diagram are presented in this chapter.

CHAPTER 2

SYSTEM DESCRIPTION

2.1 Modeling of the System

Multiple UCs, whose objective is to maximize their own pro ts, is serving the customers. The power flow direction is unidirectional while the communication infrastructure ensures a bi-directional flow of data signals. The communication channel uses Wi-Fi, LTE or Wi-MAX for data communication. Here, each day is divided into T time periods and t is the period index.

The process of electricity generation, transmission, distribution, and consumption can be segregated as generators, UCs, and customers are also known as end-users. In this work, the major focus is on the interaction between the multiple UCs and the multiple 5 customers. The customers are assumed to be comprised of EV users and those having other price elastic appliances known as demand responsive (DR) loads. An assumption is made that the EV charging takes place in residential areas only.

There can be two cases, one with single UC and the other one with multiple UCs. When there is a single UC in the grid then it is responsible to meet the charging requirements of the EV loads. But in case of multiple UCs, there will exist a competition between them, as a result, none of the UCs can be held responsible to meet all the demand. All the UCs will try to maximize their pro ts by setting their own prices and customers will decide their consumption accordingly. Game theory can be used to model and analyze the behavior of customers and of UCs in such scenarios. The UC's decide upon the price of electricity and declare it to the customers. As a response to the prices of the UCs, the customers demand an optimum amount of power [30]. Different customers behave differently so they have been modeled using different utility functions. In this work, a leader-follower Stackelberg game is designed as sequential events

where the UC’s are leaders and customers are followers. In this game, the UCs select a strategy before the customers make their decisions based on the knowledge of the customer's behavior

.

2.2 MODELLING OF ELECTRIC VEHICLES

A. How EVs are different from other traditional load

A number of EV's can be aggregated for the purpose of charging and discharging having different durations and start times. But the aggregation of EVs is different than the aggregation of traditional power resources. Giving prime importance to user satisfaction, the charging and discharging schedule needs to be decided but it still remains a major challenge due to the temporal availability of EVs. The salient feature of an EV is its capability to act as a load to the grid (charging), an energy storage (ES) device, and a supplier to the grid (discharging). When they operate in discharging mode, they don’t have any shutdown cost or start-up cost, unlike conventional generating sources.

B. Specifications of EV

There are three types of EVs available in the market i.e. battery electric vehicles, city battery electric vehicles, and plugin hybrid electric vehicles. We have considered battery electric vehicles for our study.

2.7 Advantages

- Less running cost
- Bidirectional power flow ability
- Battery Backup

Types of controllers

. PI Controller: The controller used is the discrete PI controller that takes in the reference voltage and the actual voltage and gives the maximum value of the reference current depending on the error in the reference and the actual values. PI controllers are used to get the maximum value of the reference current. This figure shows that the PI controller compares the reference voltage and the actual voltage of the system. That is the DC side capacitor voltage is sensed and compared with a desired reference voltage.

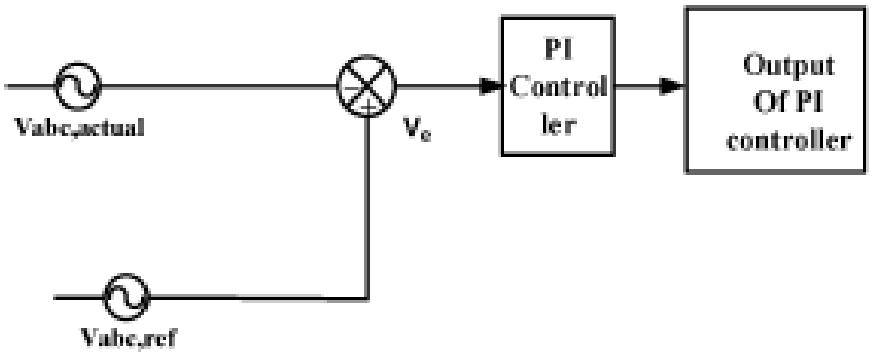

Fig. 3.1 Block diagram of PI controller

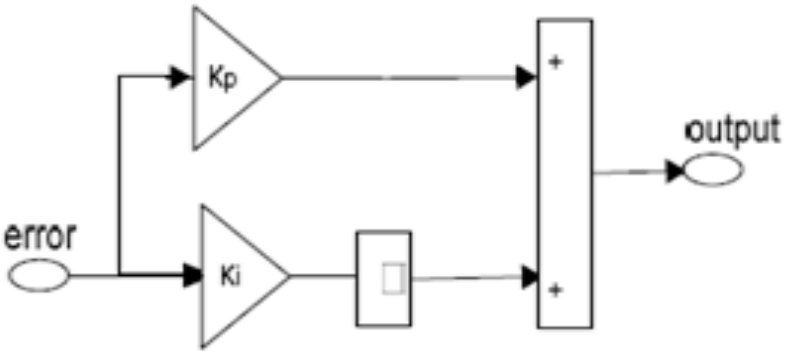

Fig. 3.2 PI Controller

Fig. 3.2. Represents the control scheme consists of a PI controller, a limiter, and a three phase sine wave generator for reference current and switching signal generation.

FOPID controller

The model of FOPID was developed from fractional differentiation. The response with PR is faster than that of the corresponding PI controlled system. A block-diagram that signifies the PR-control structure is displayed in Fig2. The transfer function of an FOPID controller takes the form of

$$C_{PR}(s)=K_P+K_I/s^{\lambda}+K_D s^{\mu}$$

where λ is the order of the integral part, μ is the order of the derivative part, while K_P, K_I, and K_D are the controller as in a conventional PID-controller.

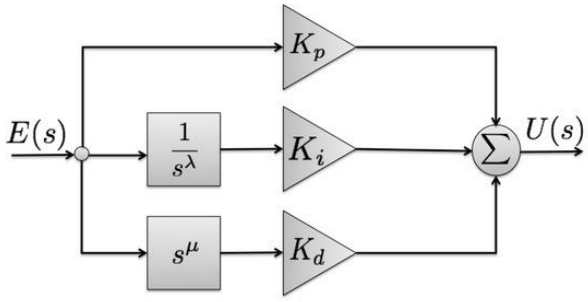

Figure 3.3 Block-diagram of FOPID-controller

2.9 Summary

The block diagram of the closed loop system and the different types of controllers are presented in this chapter.

CHAPTER 3

SIMULATION RESULTS OF OPEN LOOP ESEV SYSTEM

3.1 General

This chapter deals with the results of the open loop system. The simulation results in the forward and the reverse direction are presented in this chapter.

Simulation has become a very powerful tool in the industry application as well as in academics, nowadays. It is now essential for an electrical engineer to understand the concept of simulation and learn its use in various applications. Simulation is one of the best ways to study the system or circuit behavior without damaging it. The tools for doing the simulation in various fields are available in the market for engineering professionals.

Many industries are spending a considerable amount of time and money in doing simulation before manufacturing their product. In most of the research and development (R&D) work, the simulation plays a very important role. Without simulation, it is quite impossible to proceed further. It should be noted that in power electronics, computer simulation and a proof of concept hardware prototype in the laboratory are complementary to each other. However, computer simulation must not be considered as a substitute for hardware prototype. The objective of this chapter is to describe the simulation of impedance source inverter with R, R-L and RLE loads using MATLAB tool.

Many industries are spending a considerable amount of time and money in doing simulation before manufacturing their product. In most of the research and development (R&D) work, the simulation plays a very important role. Without simulation, it is quite impossible to proceed further. It should be noted that in power electronics, computer simulation and a proof of concept hardware prototype in the laboratory are complementary to each other. However, computer simulation must not be considered as a substitute for hardware prototype. The

objective of this chapter is to describe the simulation of impedance source inverter with R, R-L and RLE loads using MATLAB tool.

3.2 NBC-VSI fed induction Motor

The block diagram of NBC-VSI fed induction Motor in forward mode is shown in Figure 3.1.The DC from PV system is stepped up using non - isolated boost DC to DC converter. The output of NBC is converted to three phase AC using Three phase inverter. The output of TPI is applied to three phase induction motor.

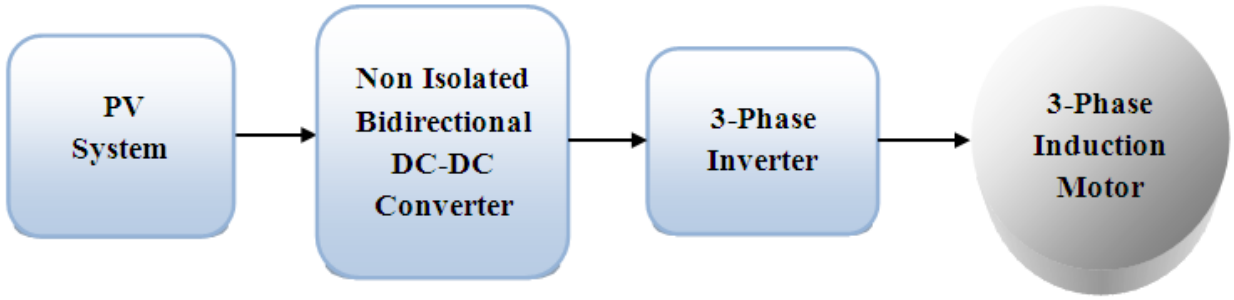

Fig 3.1 Block Diagram of NBC-VSI fed induction Motor in Forward Mode

Simulation Results

3.2.1 Bi-directional VSI fed induction motor with PV alone

The Circuit diagram of Bi-directional VSI fed induction motor with PV is appeared in Fig 3.2. The Output voltage of the solar system is shown in Fig 3.3 and its value is 60 V. The Output voltage of the bi-directional converter is shown in Fig 3.4 and its value is 390 V. The Switching pulse for M1 and M2 of the bi-directional converter are shown in Fig 3.5. The Switching pulses for M1, M2, & M5 of the inverter are shown in Fig 3.6.

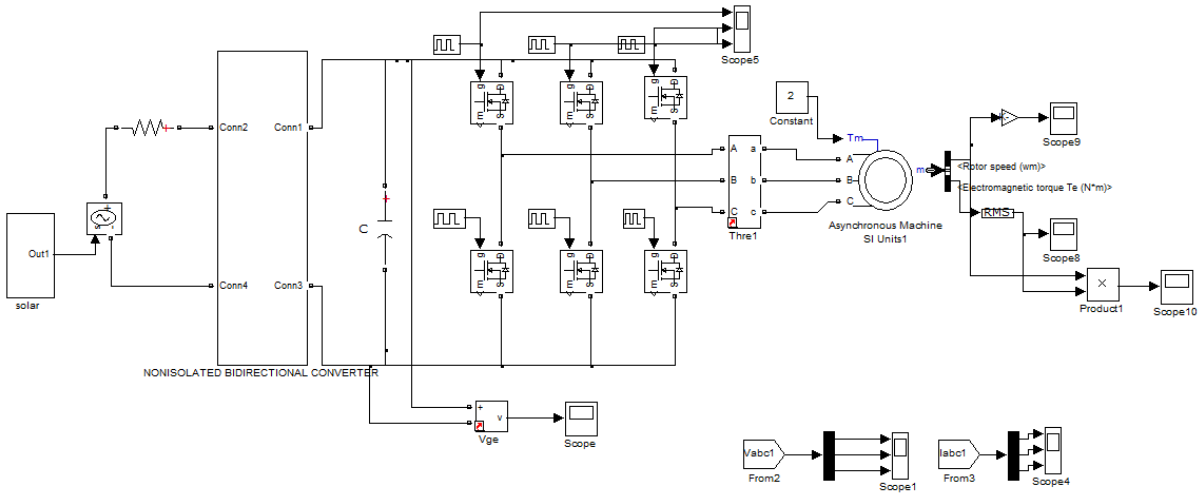

Fig 3.2 Bi-directional VSI fed induction motor with PV

The Simulink diagram shows the operation of 3 phase VSI fed supplying a motor load with solar alone as a source

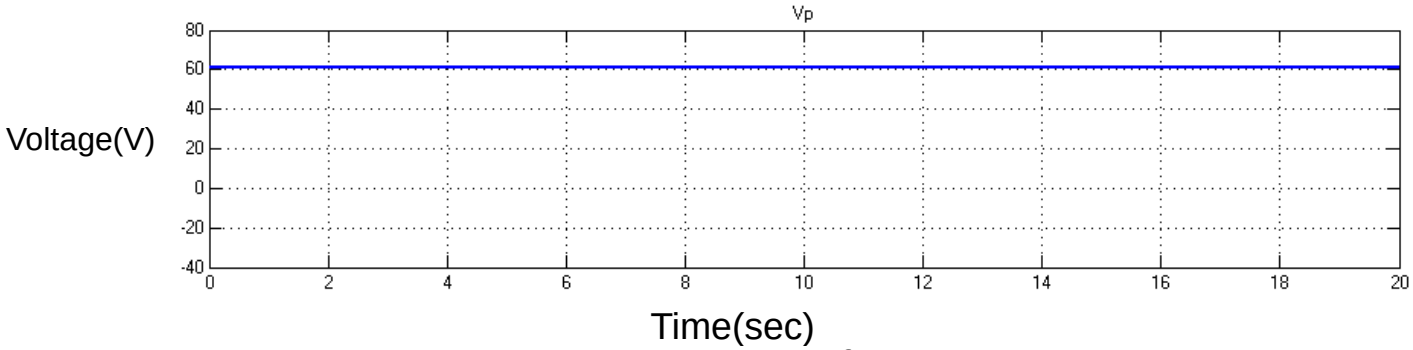

Fig 3.3 Output voltage of the solar panel

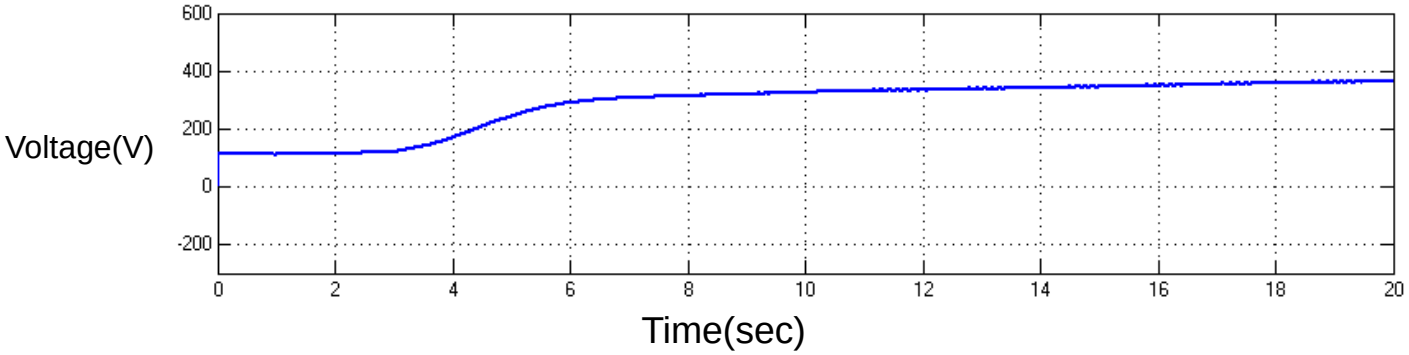

Fig 3.4 Output voltage of the bi-directional converter

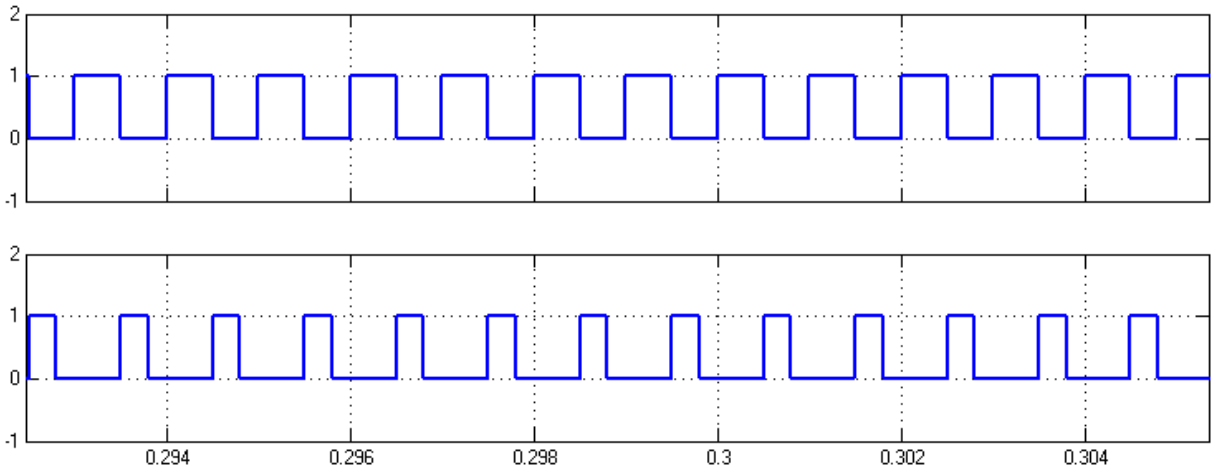

Fig 3.5 Switching pulses for M1 and M2 of the bi-directional converter

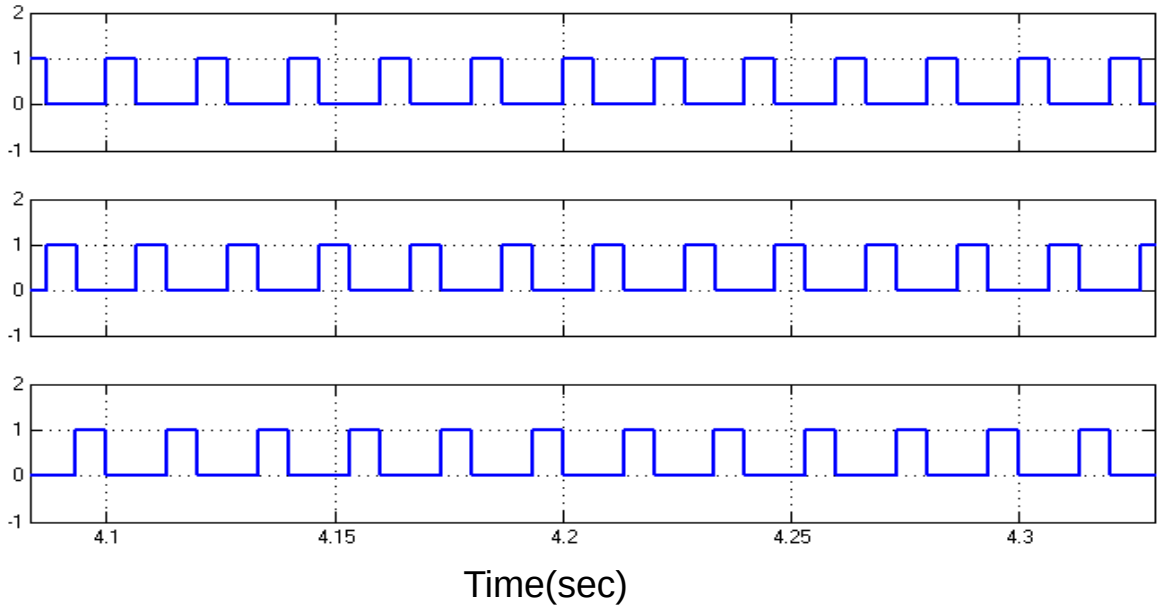

Fig 3.6 Switching pulses for M1, M2,& M5 of the inverter

The Output voltage of the inverter is shown in Fig 3.7 and its value is 450V. The Output current of the inverter is shown in Fig 3.8 and its value is 15 A. The Motor speed is shown in Fig 3.9 and its value is 1300 RPM. The Torque Response is shown in Fig 3.10 and its value is 3.5 N-m. The Output power is shown in Fig 3.11 and its value is 500 Watts.

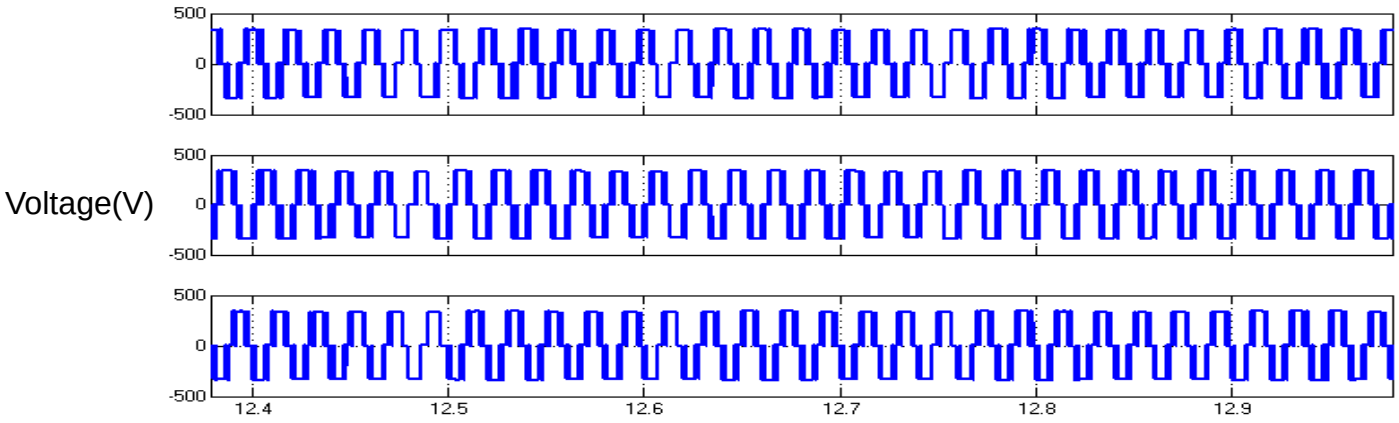

Fig 3.7 Output voltage of the inverter

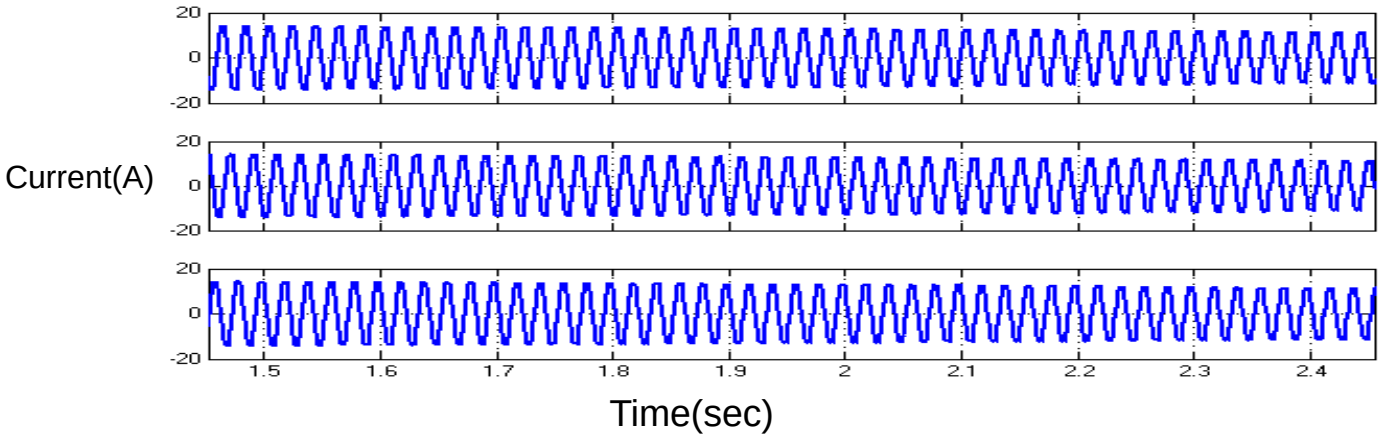

Fig 3.8 Output current waveforms

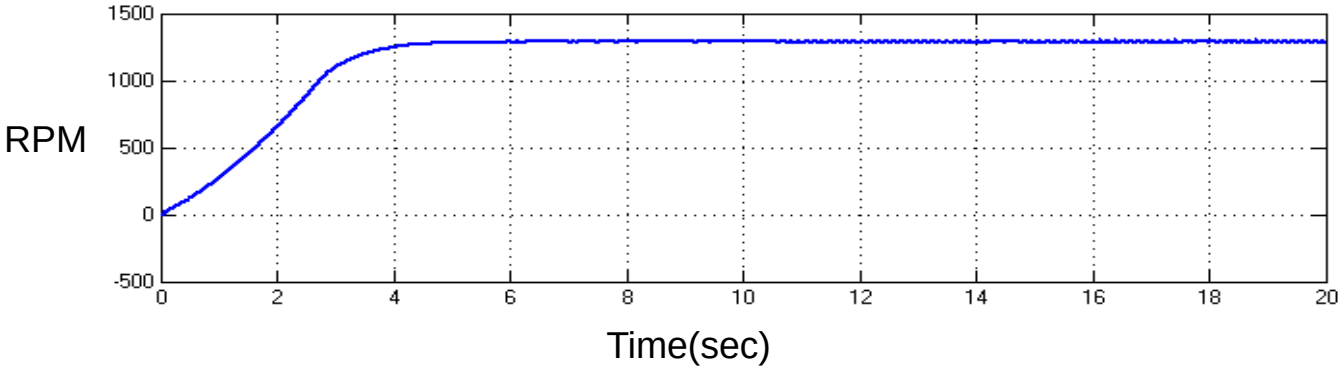

Fig 3.9 Motor speed

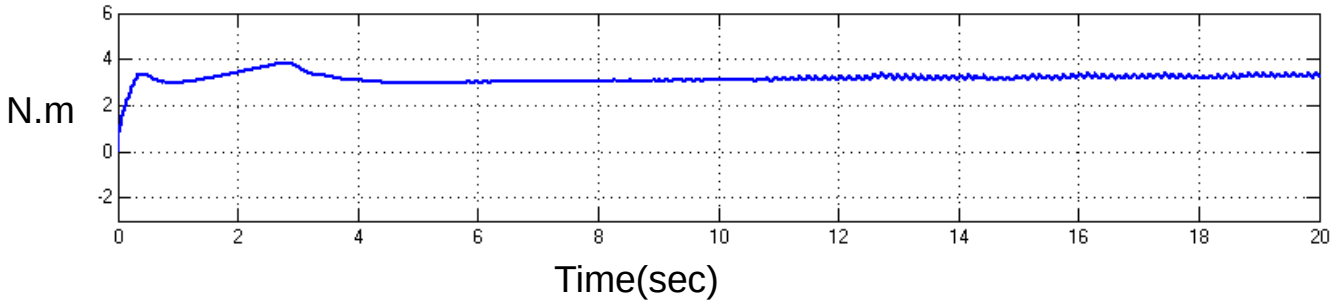

Fig 3.10 Torque Response

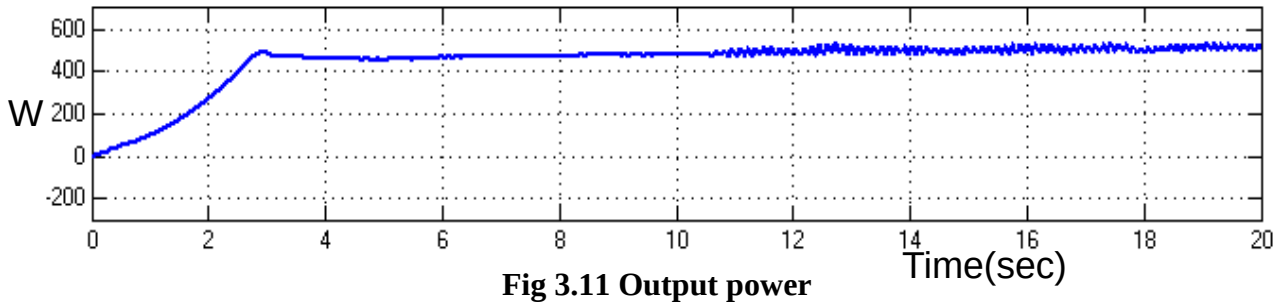

Fig 3.11 Output power

3.2.3 Battery fed NBC-VSI fed induction Motor

The block diagram of battery fed NBC-VSI fed induction Motor is shown in Figure 3.12.1.The DC from battery is stepped up using non - isolated boost DC to DC converter. The output of NBC is converted to three phase AC using three phase inverter. The output of TPI is applied to three phase induction motor.

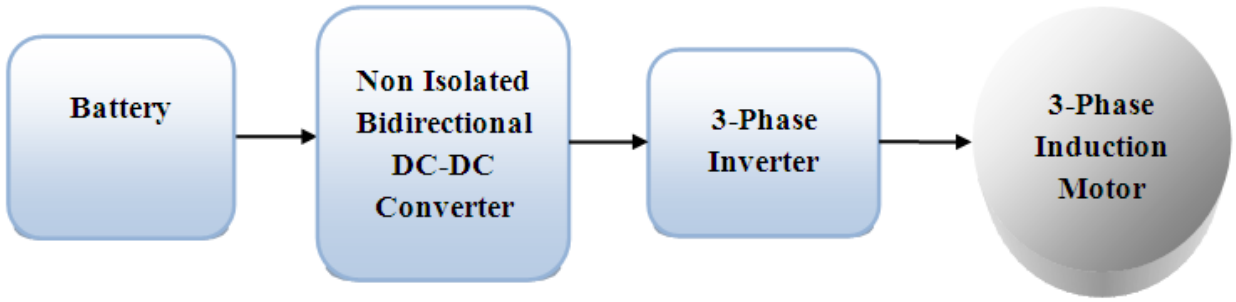

Fig 3.12.1 Battery powered NBC-VSI fed induction Motor

3.4.2 Bi-directional VSI fed induction motor with battery as a source

The circuit diagram of the Bi-directional VSI fed induction motor with Battery is shown in Fig 3.12. The Output voltage of the battery is shown in Fig 3.13 and its value is 75 V. The Output voltage of the bi-directional converter is shown in Fig 3.14 and its value is 395 V. The Output voltage of the inverter is appeared in Fig 3.15 and its peak to peak value is 350 V. The Output current of the inverter is shown in Fig 3.16 and its value is 18 A. The Motor speed is shown in Fig 3.17 and its value is 1300 RPM. The Torque Response is shown in Fig 3.18 and its value is 3.5 N-m. The output power is shown in Fig 3.19 and its value is 500 Watts.

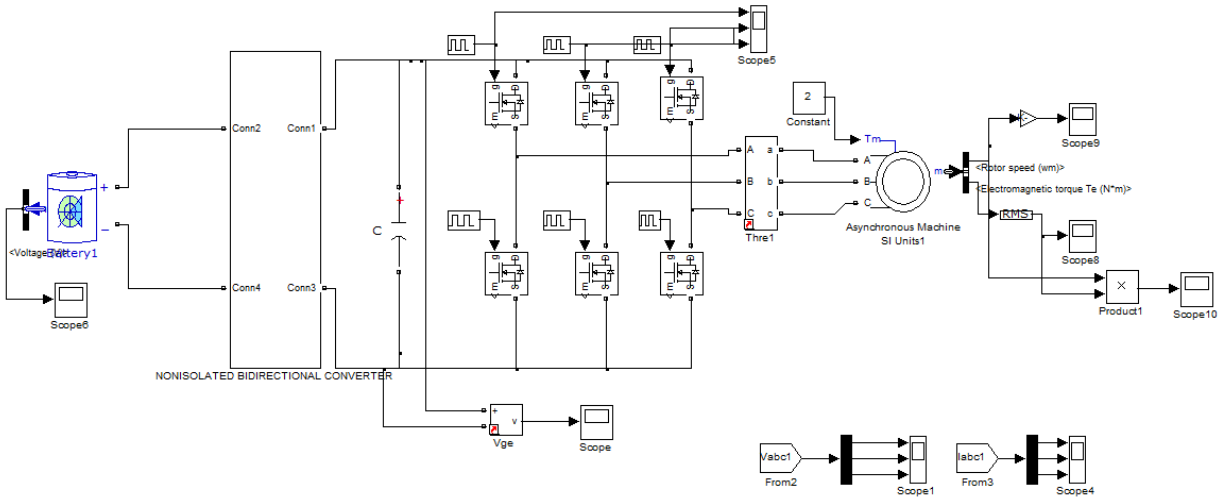

Fig 3.12 Circuit diagram of the Bi-directional VSI fed induction motor with battery

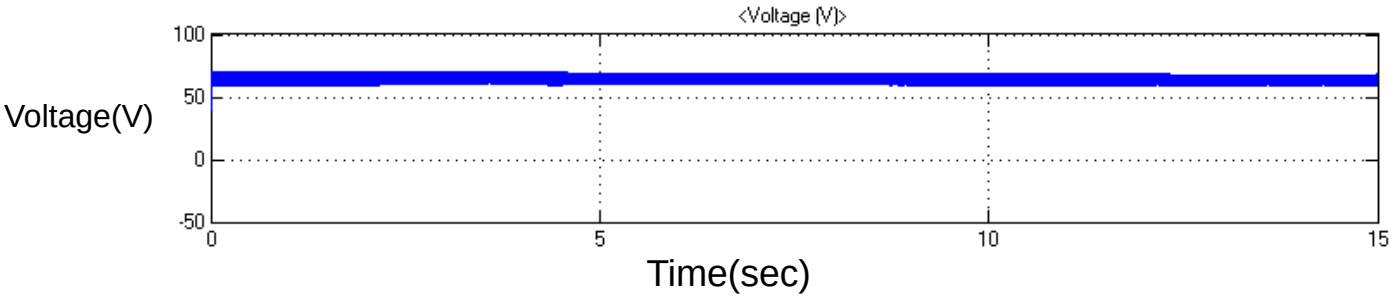

Fig 3.13 Output voltage of the battery

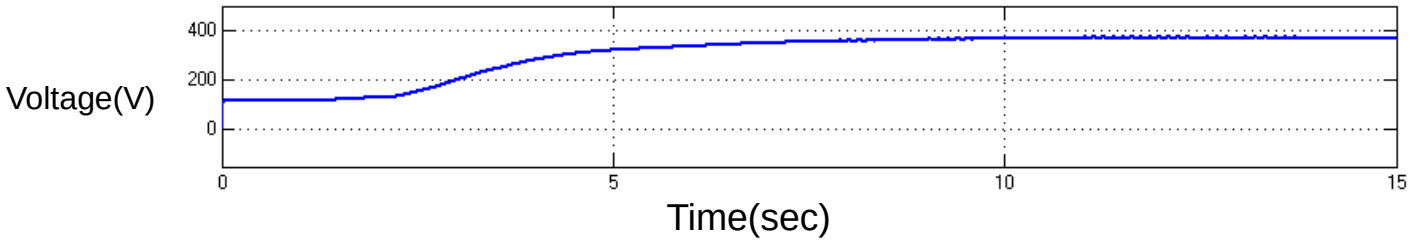

Fig 3.14 Output voltage of the bi-directional converter

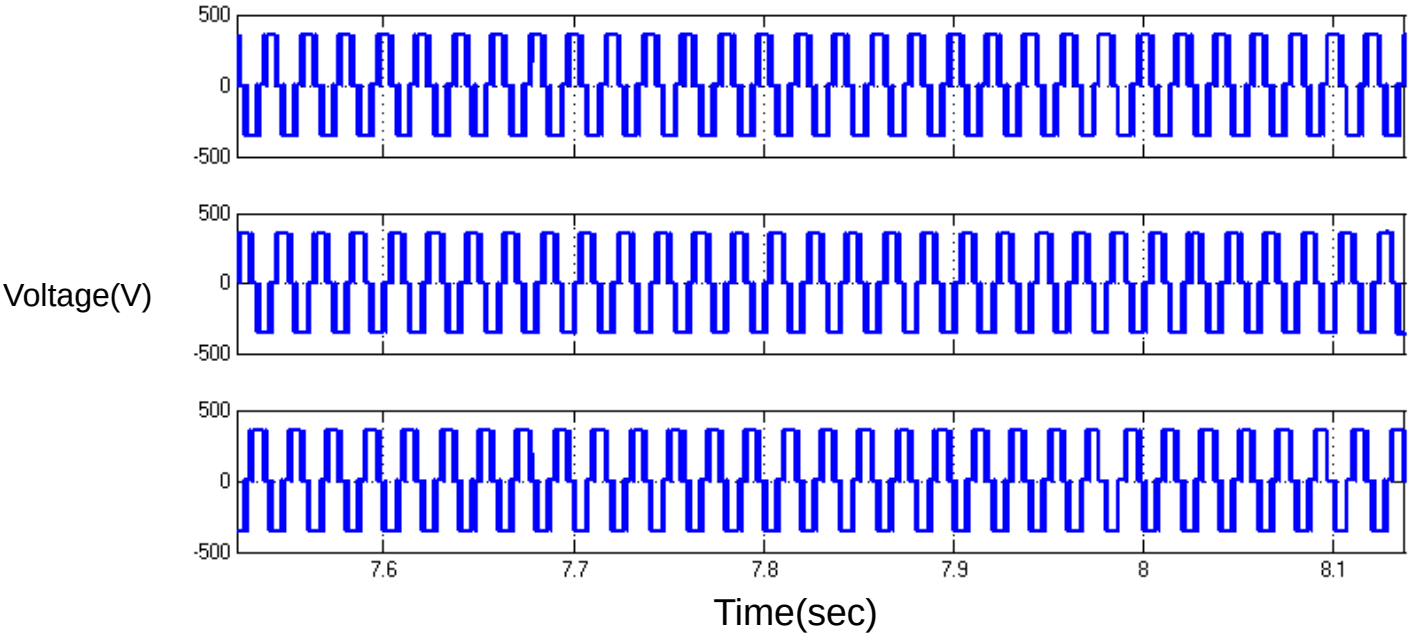

Fig 3.15 Output voltage of the inverter

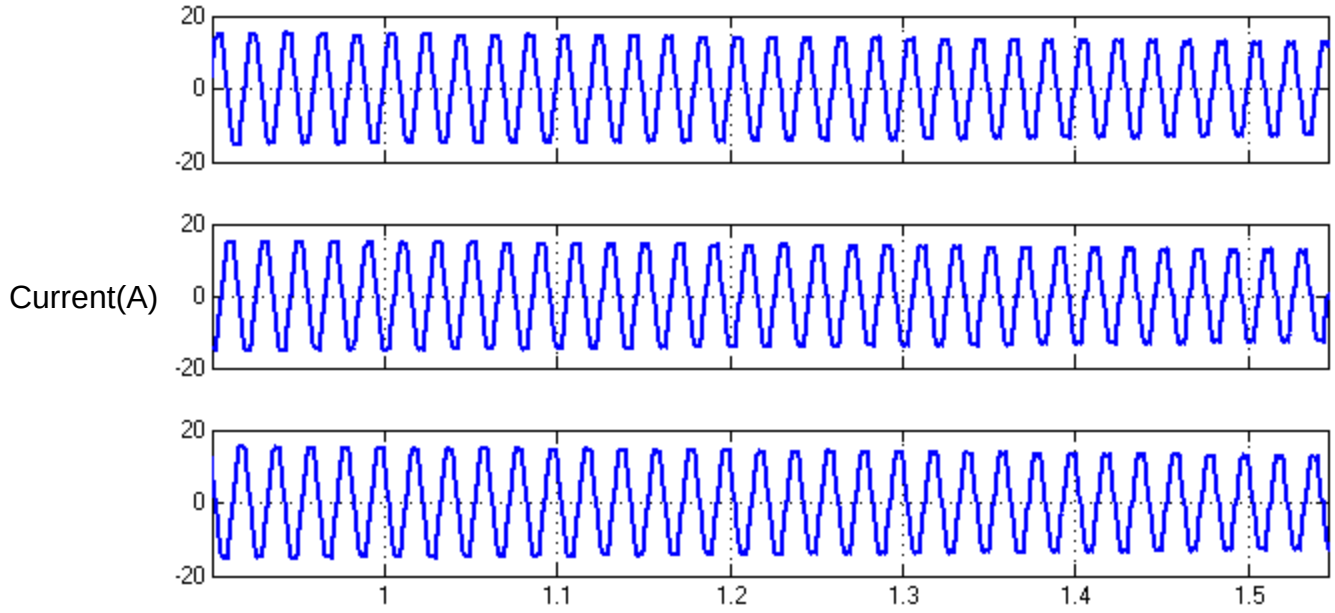

Fig 3.16 Output current of the inverter

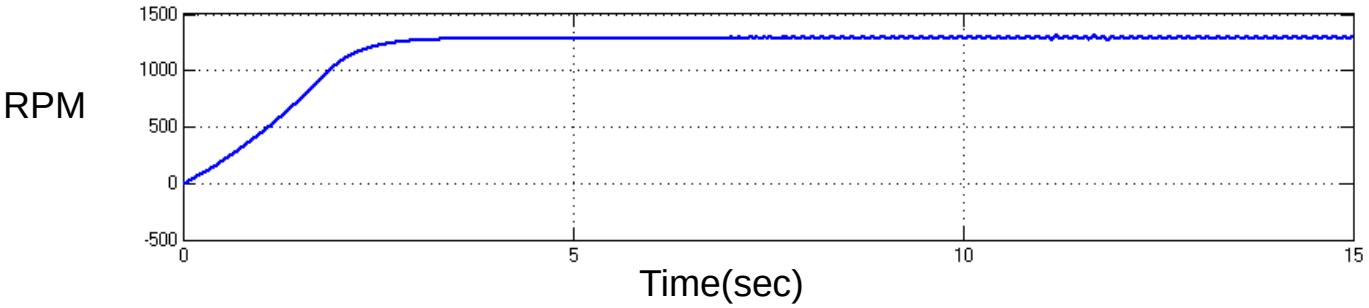

Fig 3.17 Motor speed

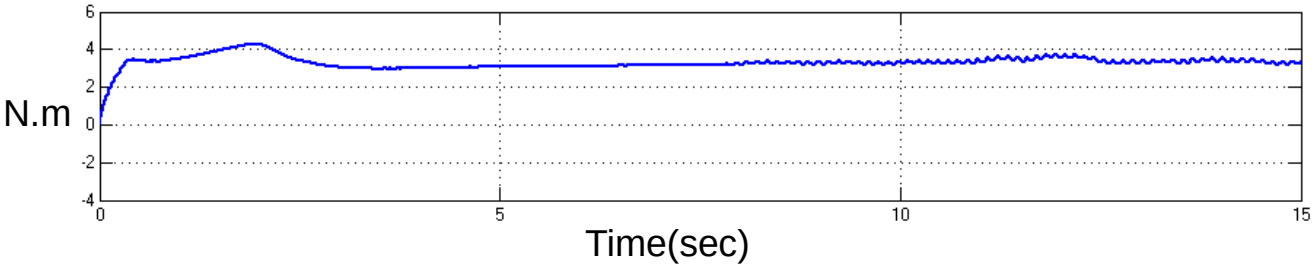

Fig 3.18 Torque Response

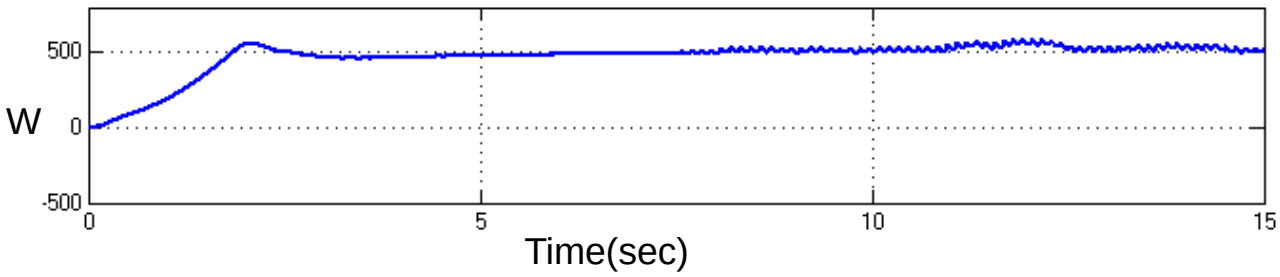

Fig 3.19 Output power

3.3 Induction Motor System with Battery and PV sources

The block diagram of Induction Motor System with Battery and PV sources is shown in Figure 3.12.1.The DC from battery and PV system is stepped up using non - isolated boost DC to DC converter. The output of NBC is converted to three phase AC using three phase inverter. The output of TPI is applied to three phase induction motor.

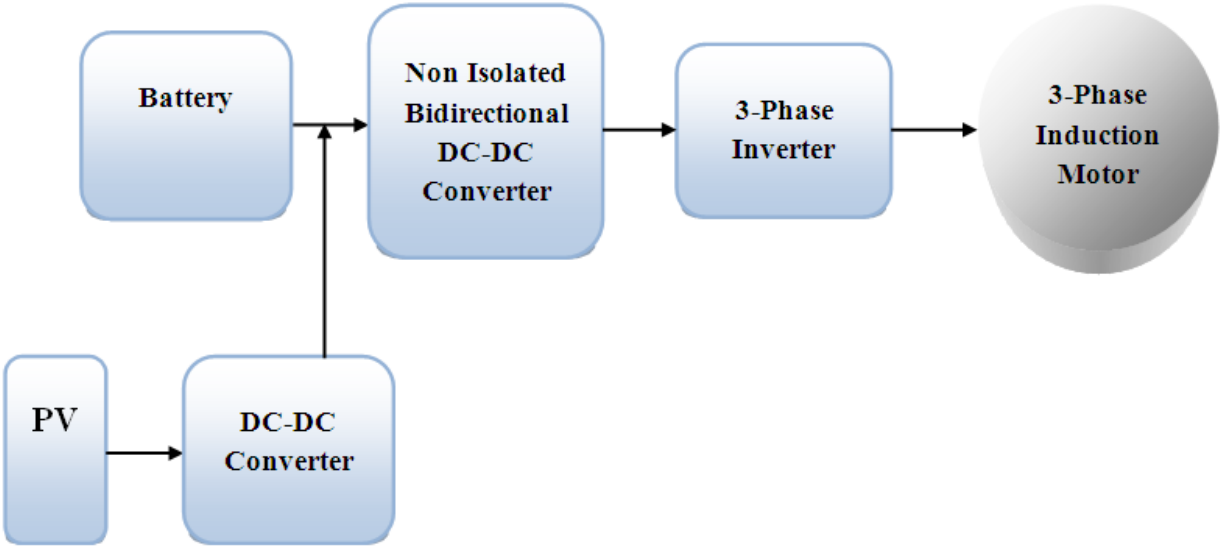

Fig 3.20.1 Induction Motor System with Battery and PV sources

3.3.2 Bi-directional VSI fed induction motor with PV & Battery

The circuit diagram of the Bi-directional VSI fed induction motor with PV & Battery is appeared in Fig 3.20. The Output voltage of the battery is shown in Fig 3.21 and its value is 70 V. The Output voltage of the solar is shown in Fig 3.22 and its value is 60 V. The circuit diagram of the Bi-directional converter is shown in Fig 3.23. The Output voltage of the bi-directional converter is shown in Fig 3.24 and its value is 400 V. The Output current of the inverter is appeared in Fig 3.25 and its peak to peak value is 450 A. The Output voltage of the inverter is shown in Fig 3.26 and its peak to peak value is 18 V. The motor speed is shown in Fig 3.27 and its value is 1450 RPM. The Torque Response is shown in Fig 3.28 and its value is 4 N-m. The output power is shown in Fig 3.29 and its value 400 Watts. The Comparison of the output voltage, Power & motor Speed is given in Table 3.1.

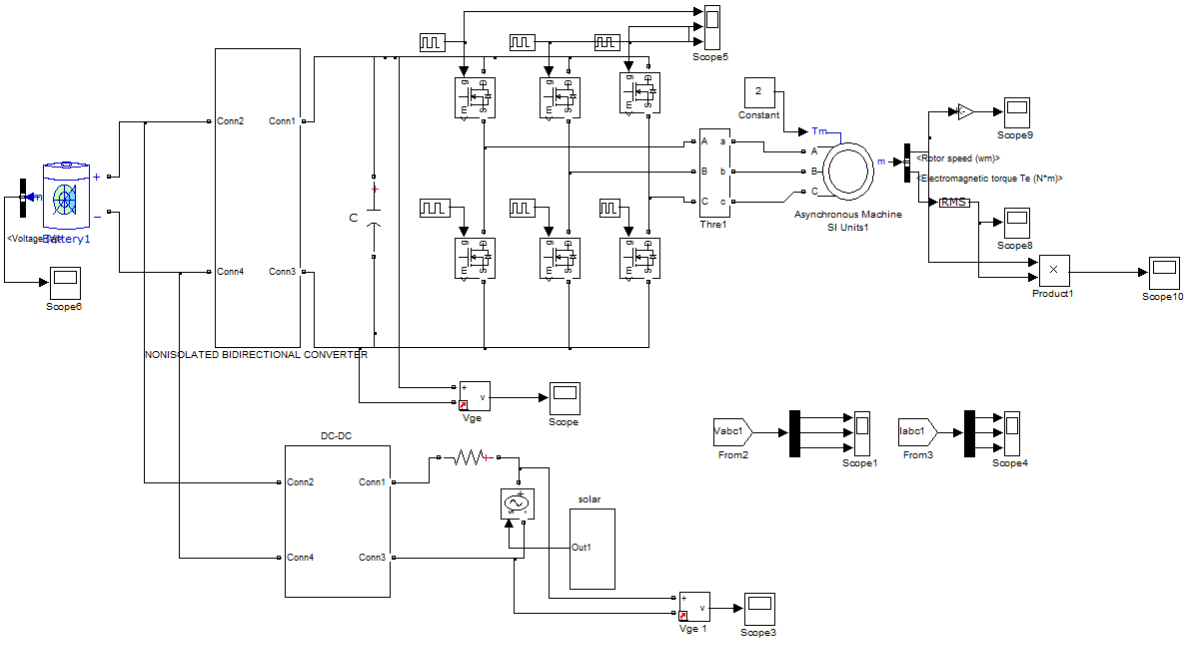

Fig 3.20 Circuit diagram of the Bi-directional VSI fed induction motor with PV & Battery

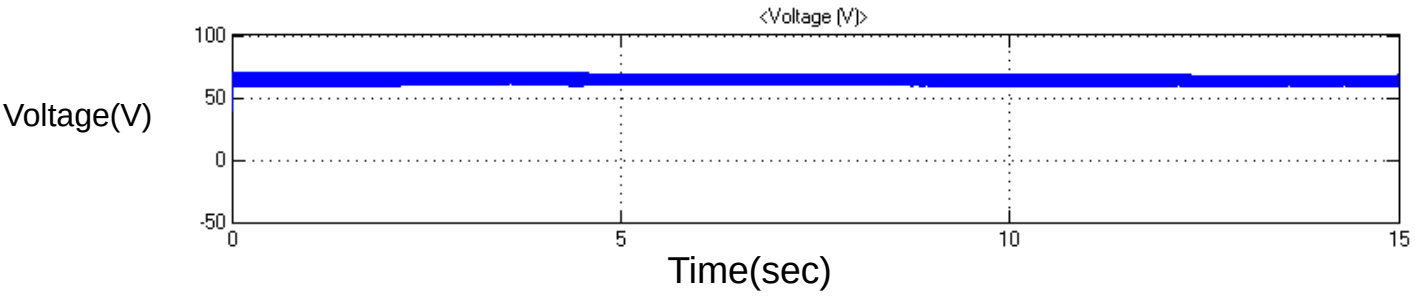

Fig 3.21 Output voltage of the battery

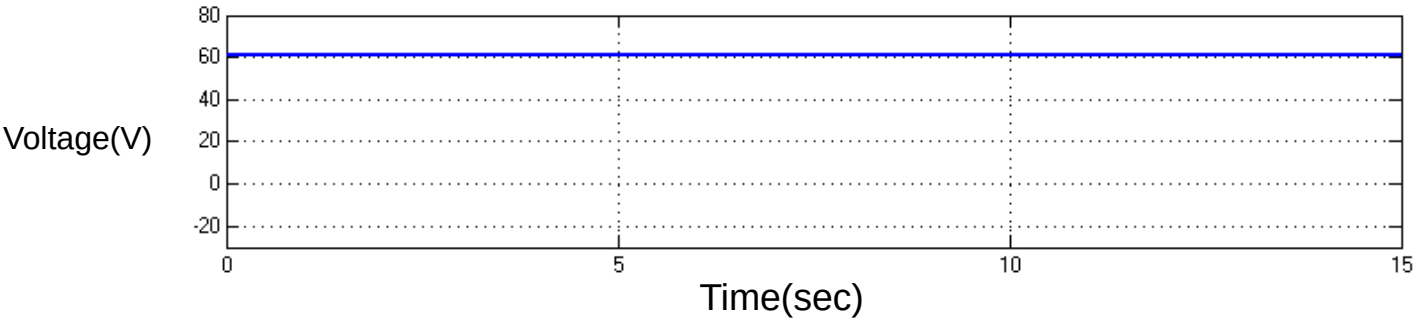

Fig 3.22 Output voltage of the solar

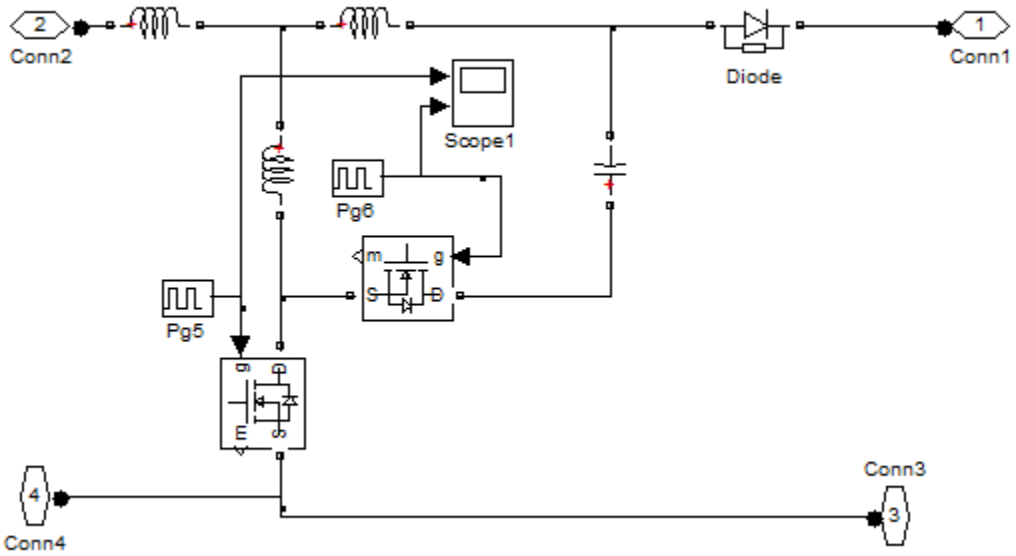

Fig 3.23 Circuit diagram of theBi-directional converter

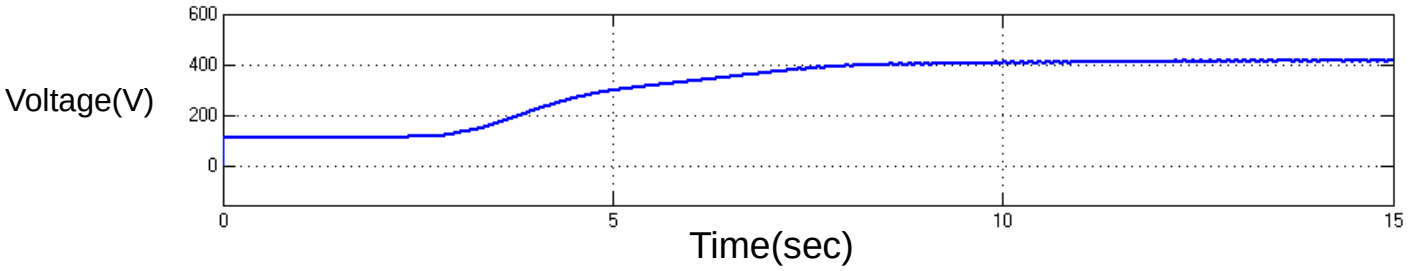

Fig 3.24 Output voltage of the bi-directional converter

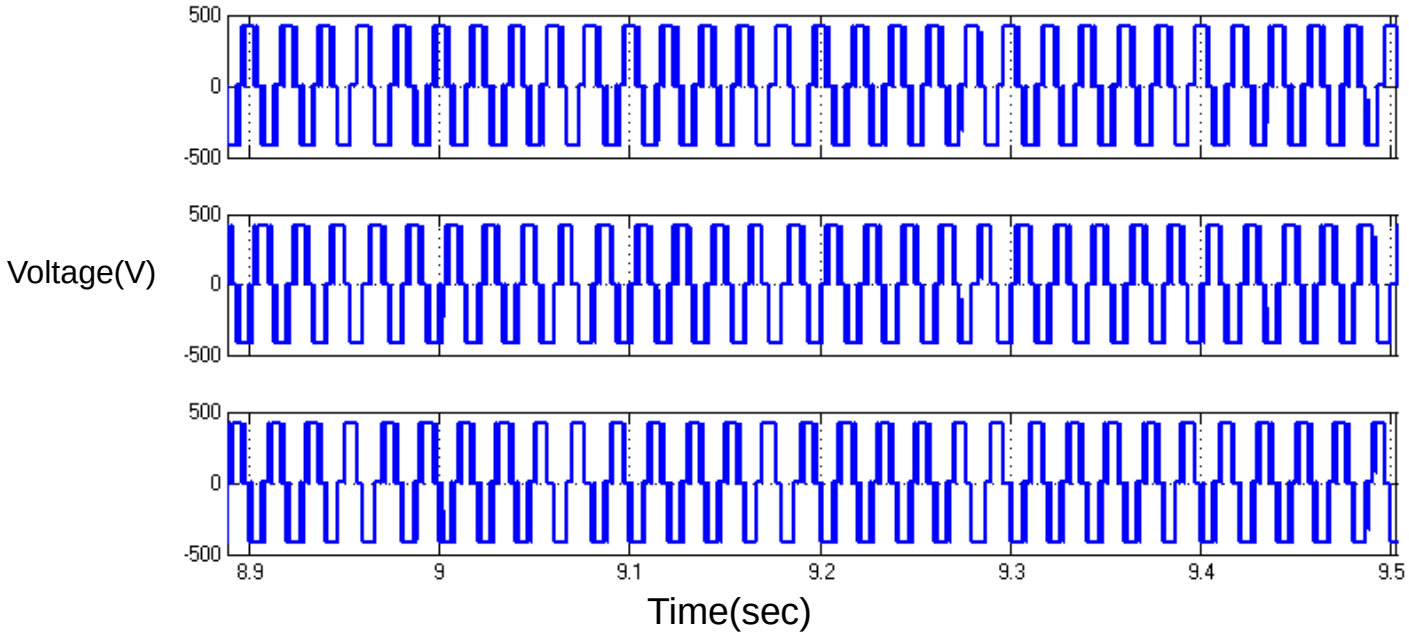

Fig 3.25 Output voltage of the inverter

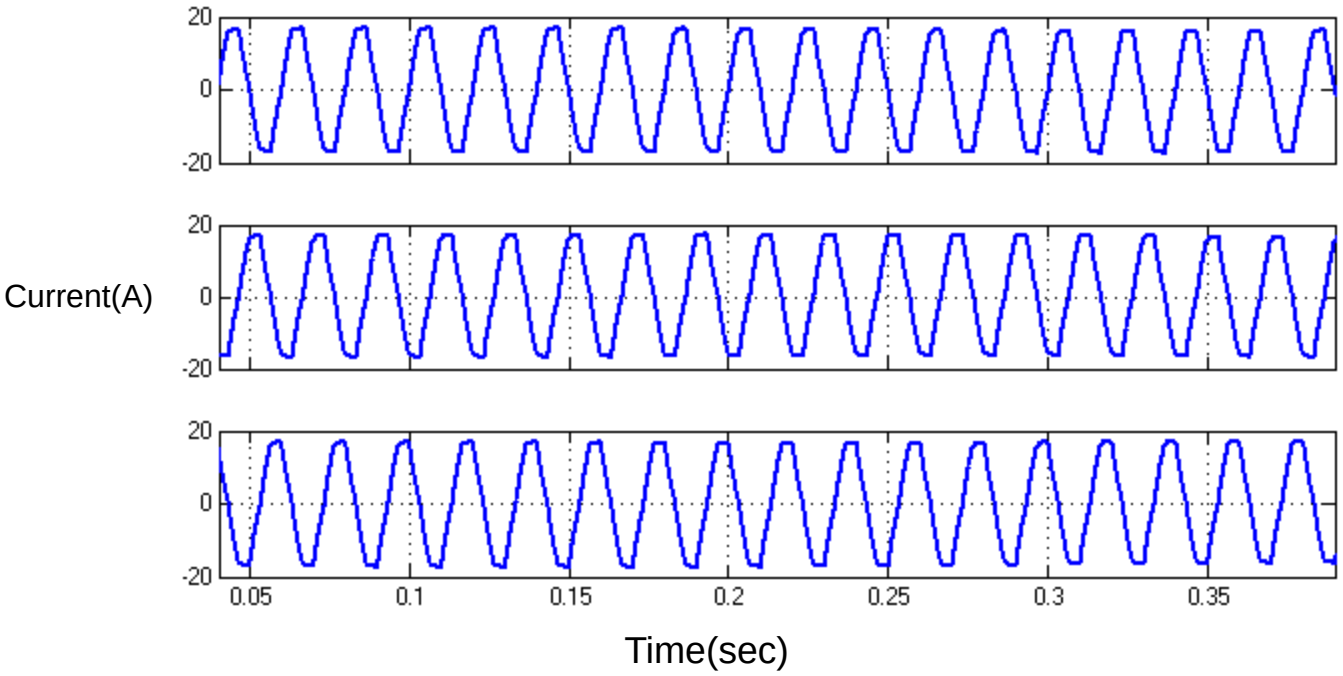

Fig 3.26 Output current of the inverter

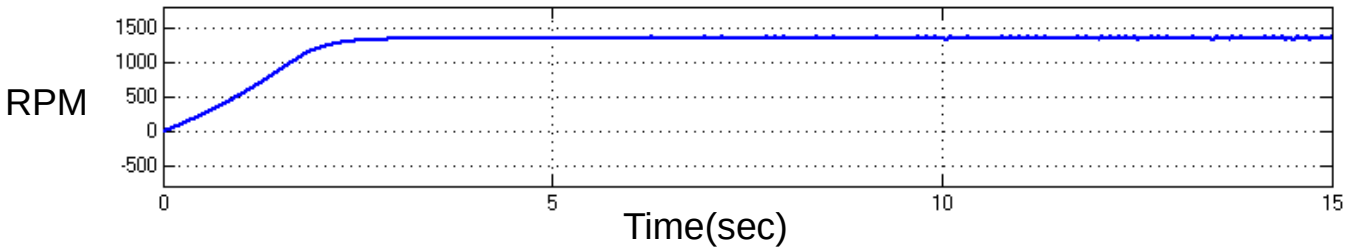

Fig 3.27 Motor speed

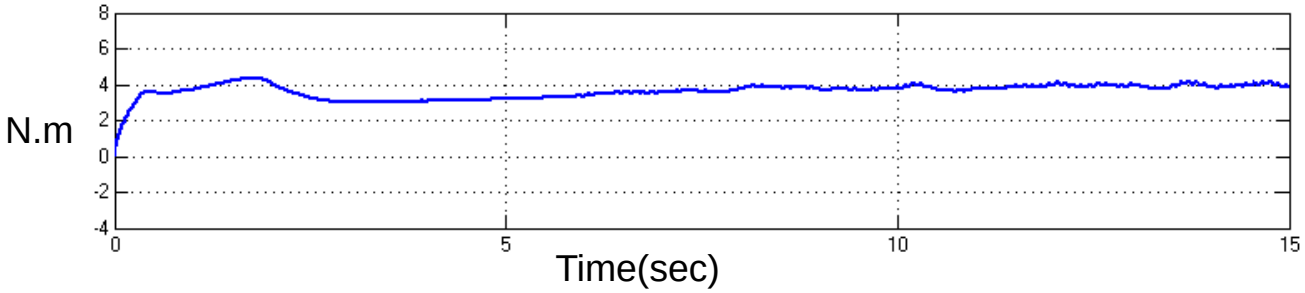

Fig 3.28 Torque Response

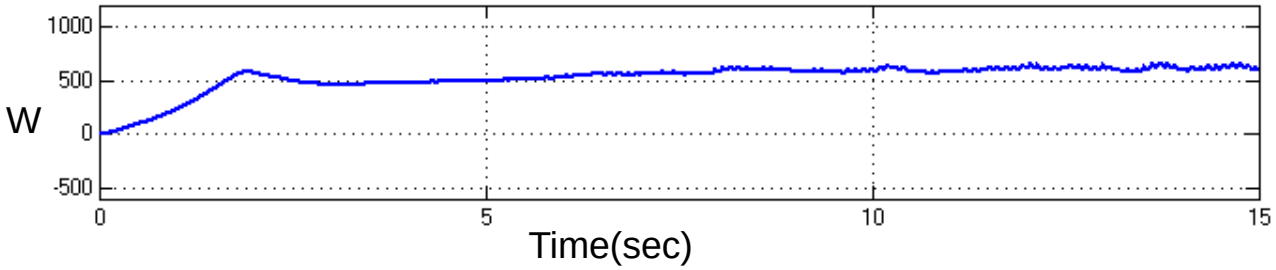

Fig 3.29 Output power

Table -3.1

Comparison of the output voltage, Power & motor Speed

Case	V_{bo}	Motor speed	Output Power
PV	360V	1290rpm	510W
Battery	375V	1300rpm	550W
Both PV & Battery	415V	1350rpm	600W

3.3.4 Bi-directional converter system in reverse mode

In reverse mode, the induction machine works as an induction generator. The output of induction generator is rectified using a rectifier. The output of rectifier is stepped up using DDC. The output of DDC is used to charge the battery.

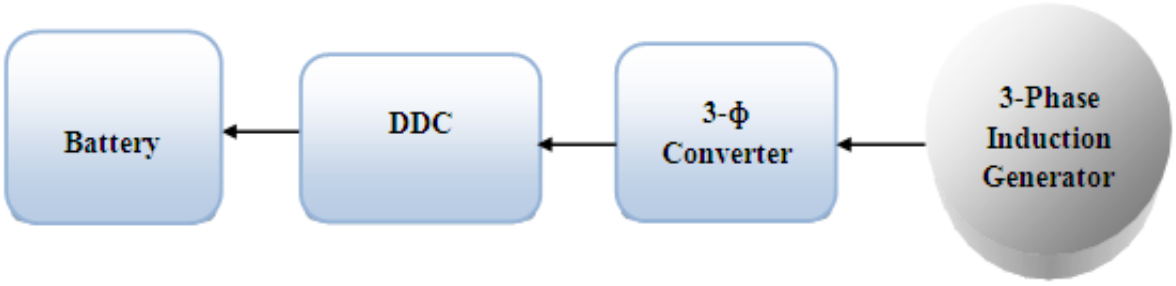

Fig 3.30.1 Bidirectional DC-DC Converter System in Reverse Mode

3.3.5 Simulation results

The circuit diagram of the Bi-directional converter in reverse mode is appeared in Fig 3.30. The input voltage is shown in Fig 3.31 and its peak value is 400 V. The Switching pulses for M1, M2, and M5 of the rectifier are shown in Fig 3.32 and its peak to peak value is 1V. The output voltage of the three-phase rectifier is shown in Fig 3.33 and its value is 400 V. The Switching pulse for M1 and M2 of the bi-directional converter are shown in Fig 3.34 and its peak to peak value is 1V. The Output voltage of the battery is shown in Fig 3.35 and its value is 95 V. The Output current of the battery is shown in Fig 3.36 and its value is 15 A. The Battery discharge curve is shown in Fig 3.37.

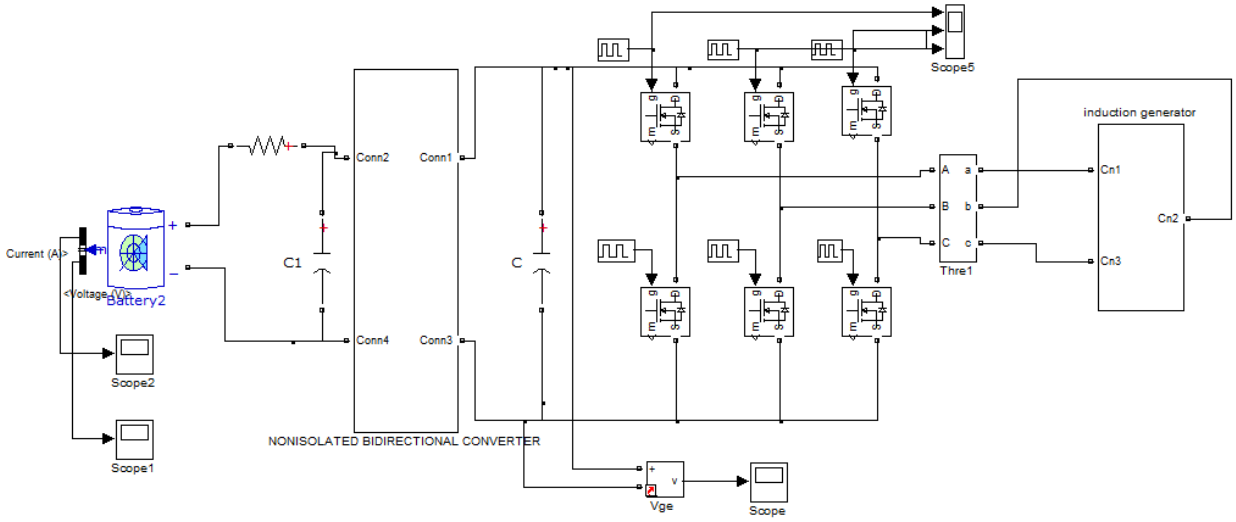

Fig 3.30 Circuit diagram of the Bi-directional converter in reverse mode

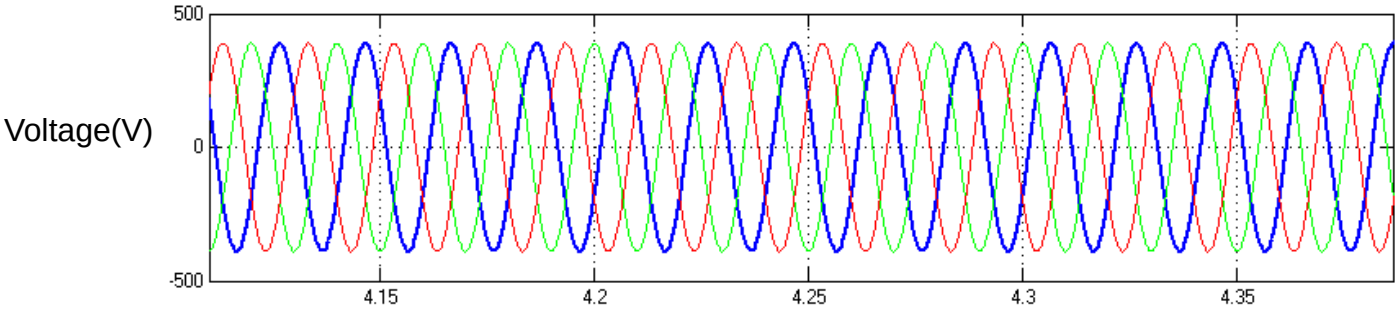

Fig 3.31 Input voltage

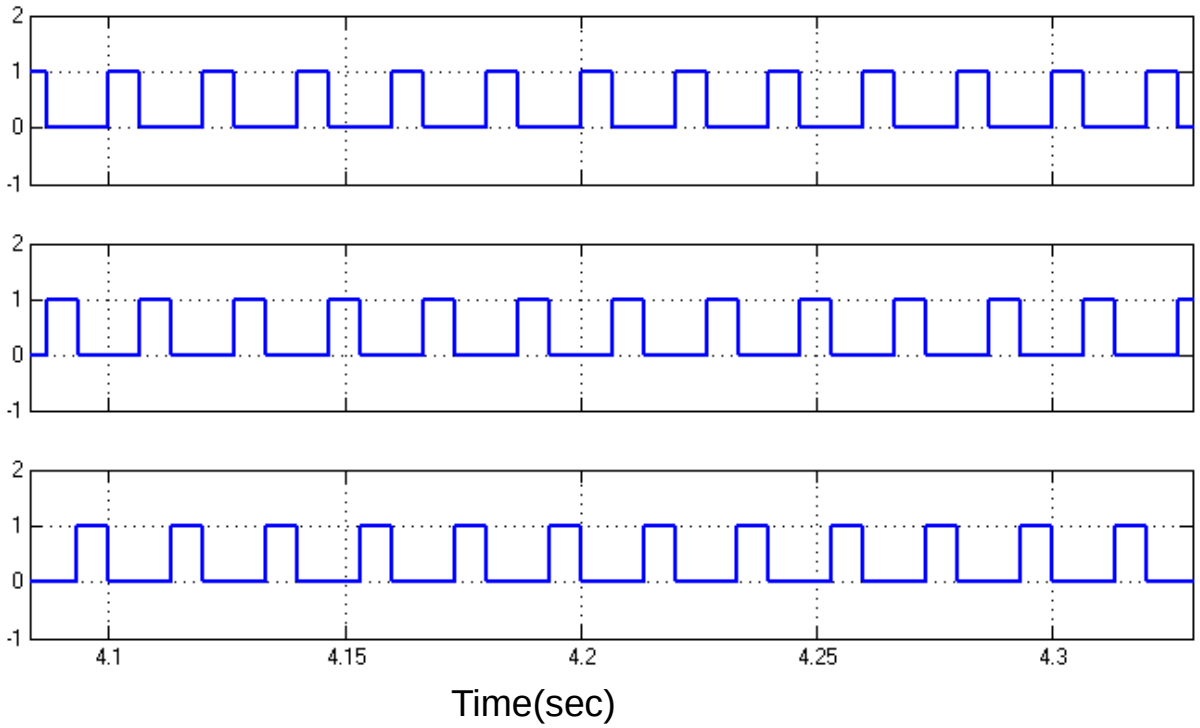

Fig 3.32 Switching pulses for M1, M2,& M5 of the rectifier

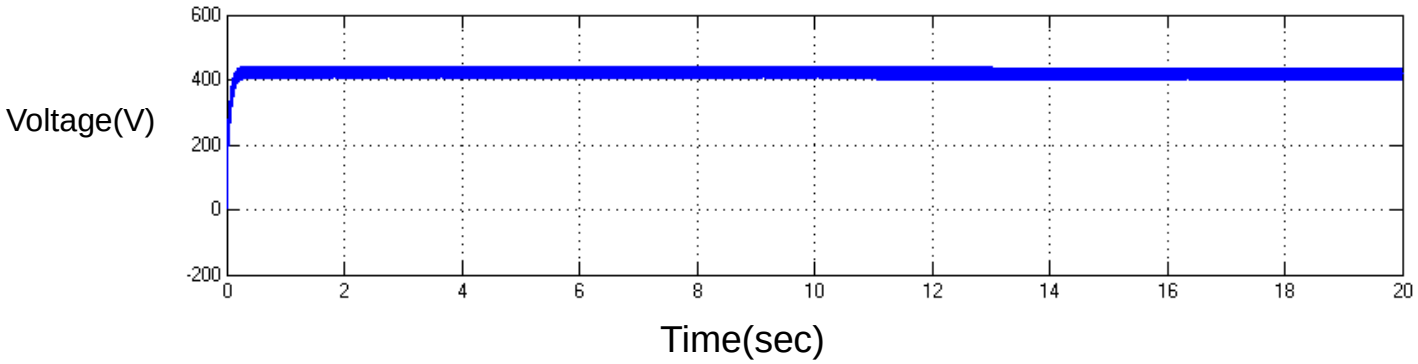

Fig 3.33 Output voltage of the three-phase rectifier

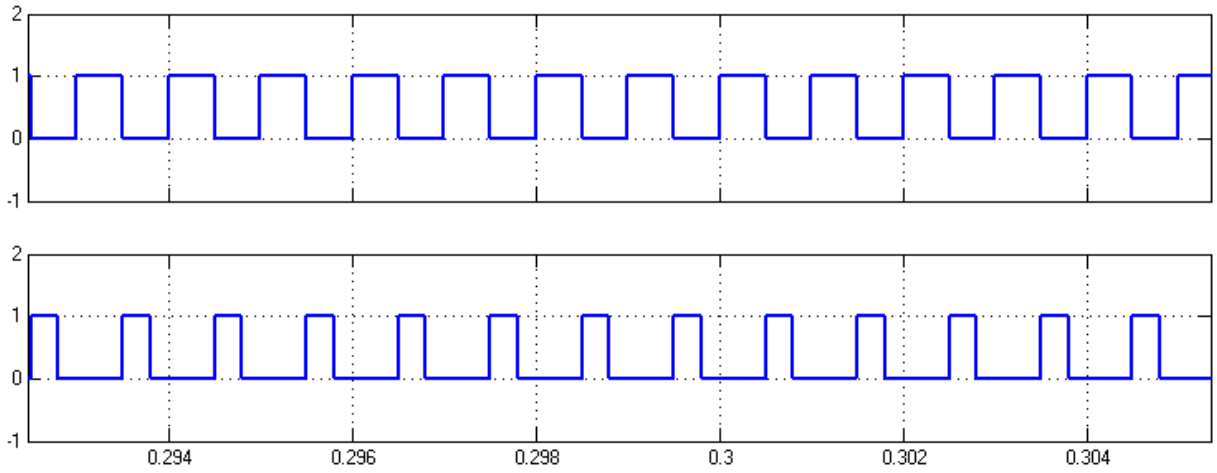

Fig 3.34 Switching pulses for M1 and M2 of the bi-directional converter

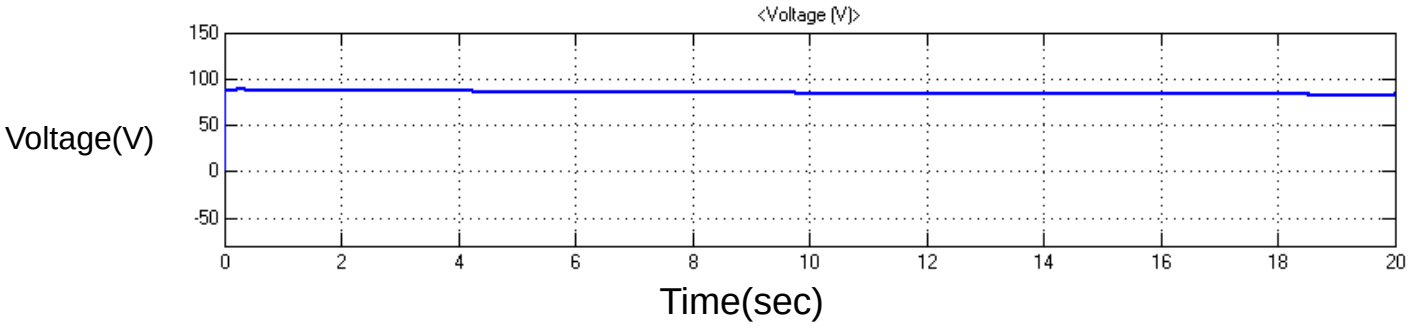

Fig 3.35 Output voltage of the battery

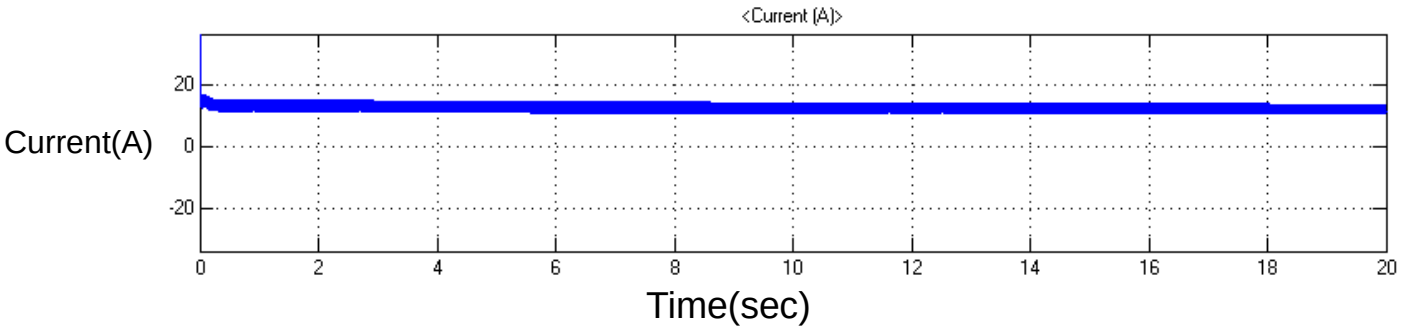

Fig 3.36 Output current of the battery

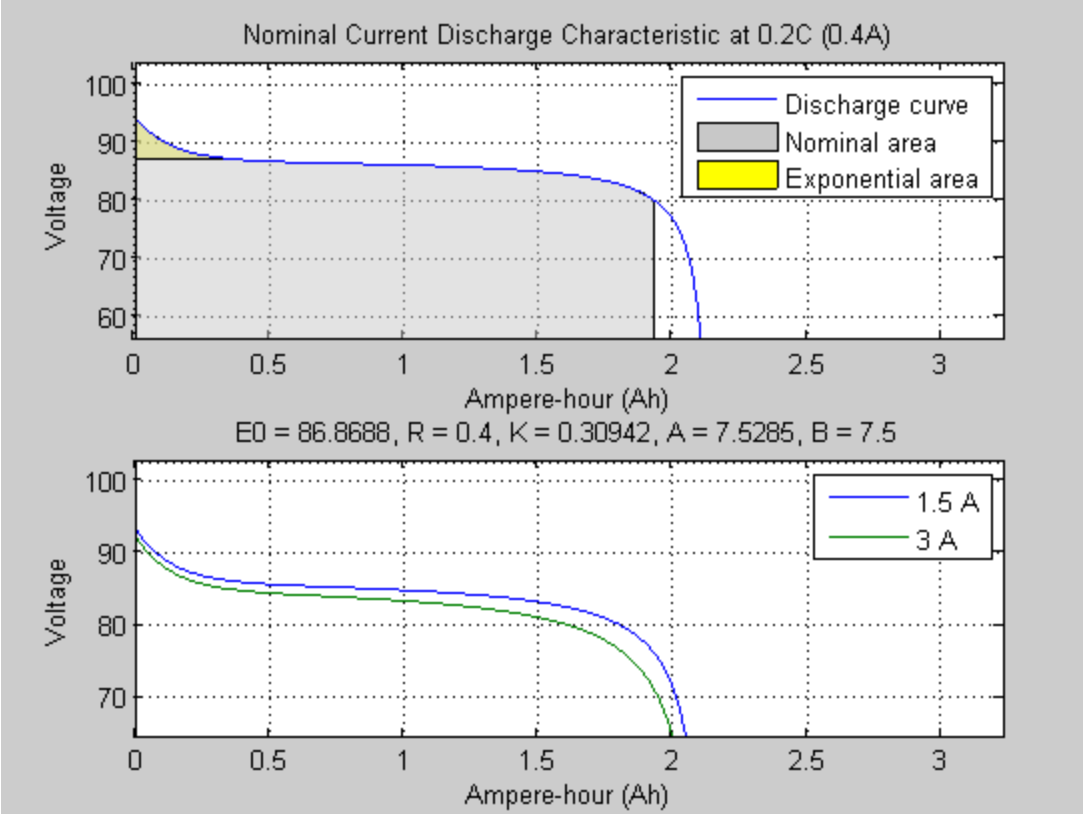

Fig 3.37 Battery discharge curve

3.4 Chapter Summary

The Bi-directional Voltage source inverter fed Induction motor with PV source in forward mode is simulated. The Bi-directional Voltage source inverter fed Induction motor with Battery source in forward mode is simulated. The Bi-directional Voltage source inverter fed Induction motor with PV and battery source in forward mode is simulated. The Bi-directional Induction generator system in reverse mode is simulated.

CHAPTER 4

CLOSED LOOP ESEV SYSTEM WITH CHANGE IN LOAD TORQUE

4.1 General

This chapter deals with results of the open-loop system with change in load torque. The comparison of results of the closed-loop system with PI, FOPID, and FLC are also presented in this chapter.

4.2 Simulation Results

4.2.1 open-loop ESEV system with change in load

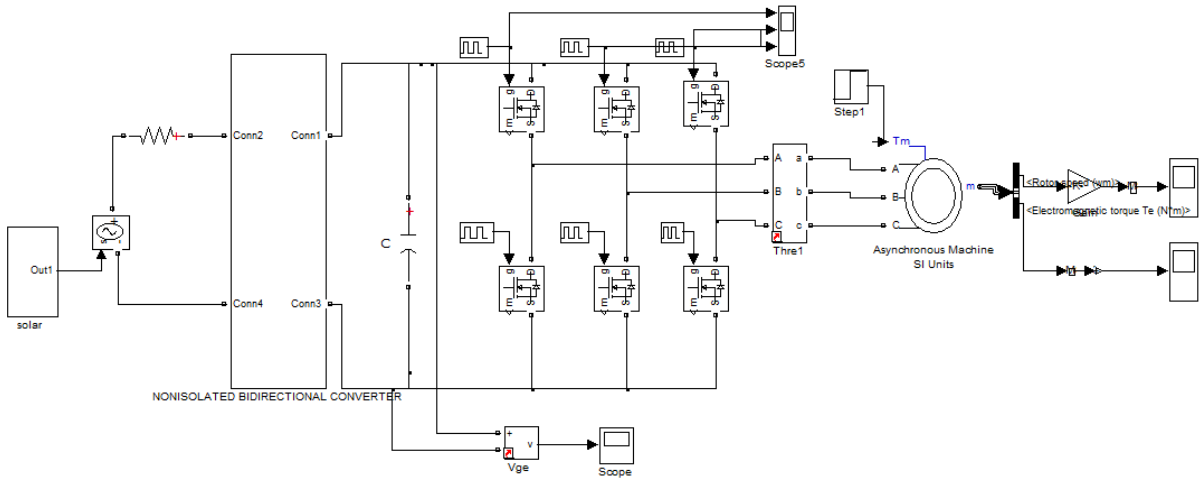

Fig 4.1 Circuit diagram of the open-loop system with change in load

The circuit diagram of the open-loop ESEV system with change in load is shown in Fig 4.1. The Motor speed is shown in Fig 4.2 and its value is 1180 RPM. The Motor speed (expanded speed waveform) is shown in Fig 4.3 and the speed reduces to 1140 RPM with increase in load. The Torque Response is shown in Fig 4.4 and its value is 1 N-m.

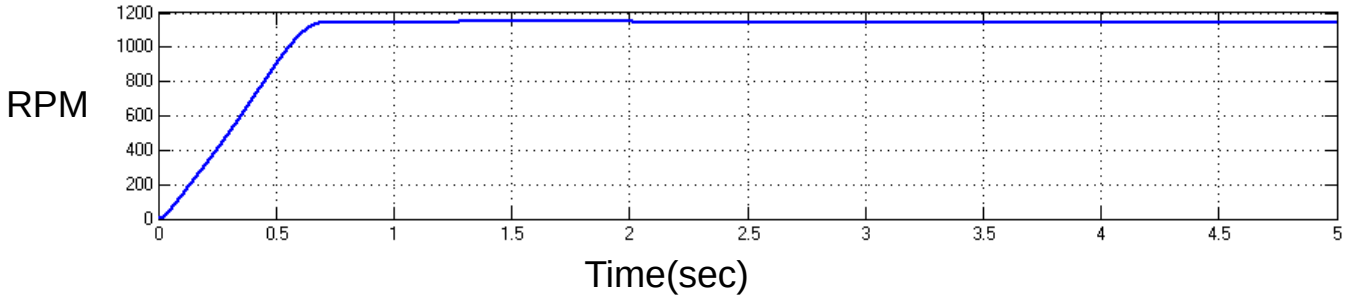

Fig 4.2 Motor speed

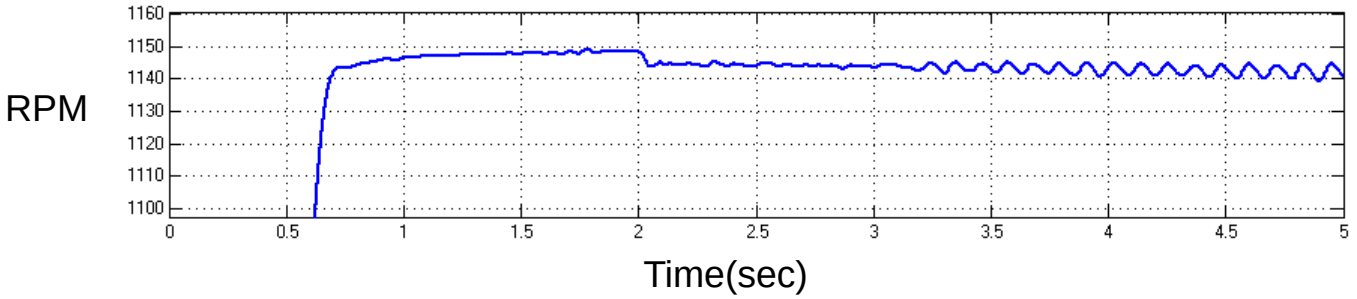

Fig 4.3 Motor speed (expanded speed waveform)

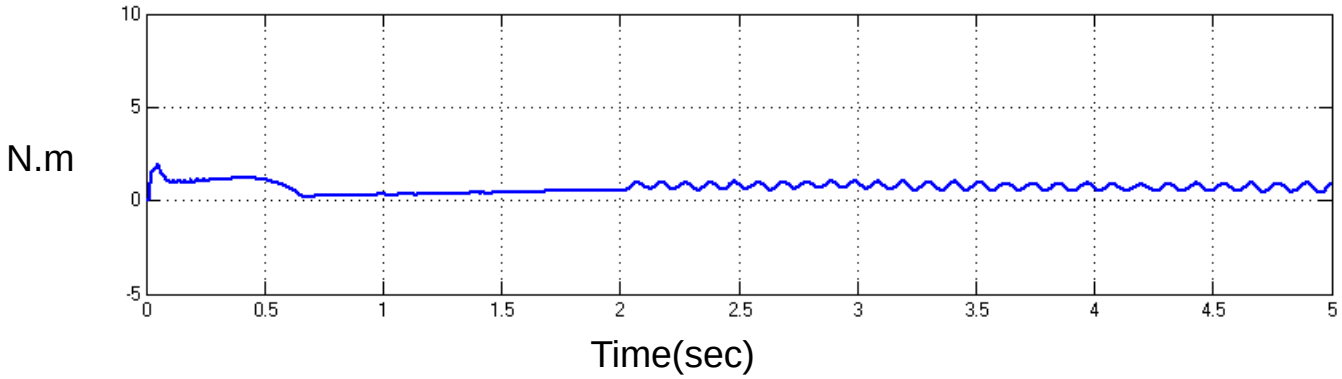

Fig 4.4 Torque Response

4.2 .2 Closed-loop ESEV system with PI controller

The point of this work is to redress enhancement of time response of IM system using PI controller. The VSI is then used to control the speed of the drive by fluctuating the AC voltage. The DC voltage is controlled by utilizing PI to regulate the speed. The Block Diagram of PI controlled IMD system is shown in Fig.4.5.1. The flow chart for PI controlled IMD system is shown in Fig.4.5.2.

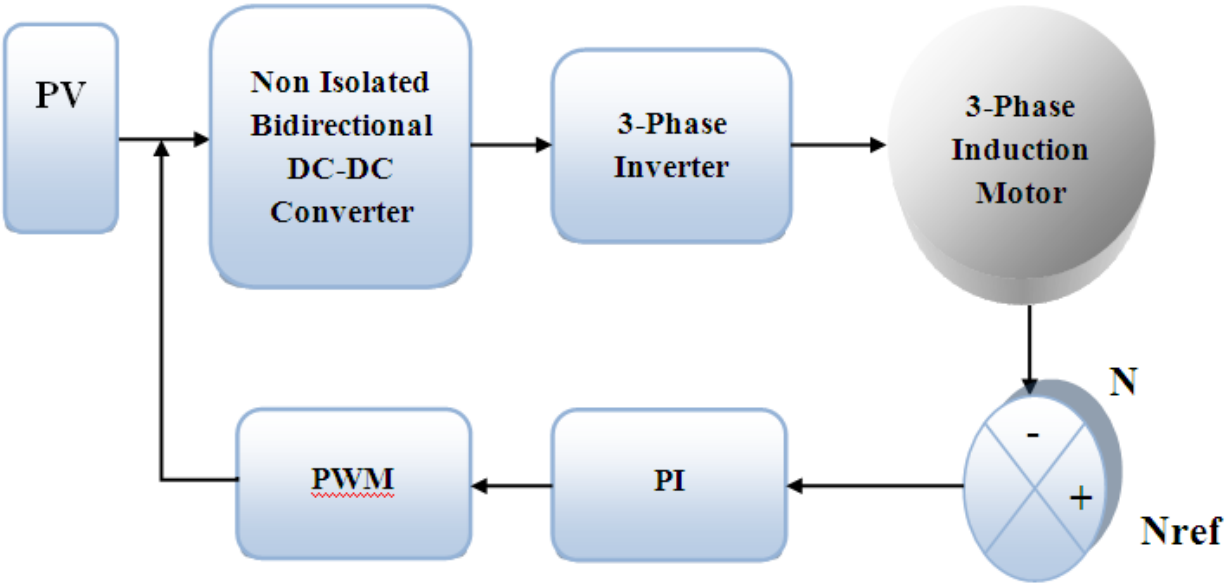

Fig 4.5.1 Closed loop ESEV system with PI converter

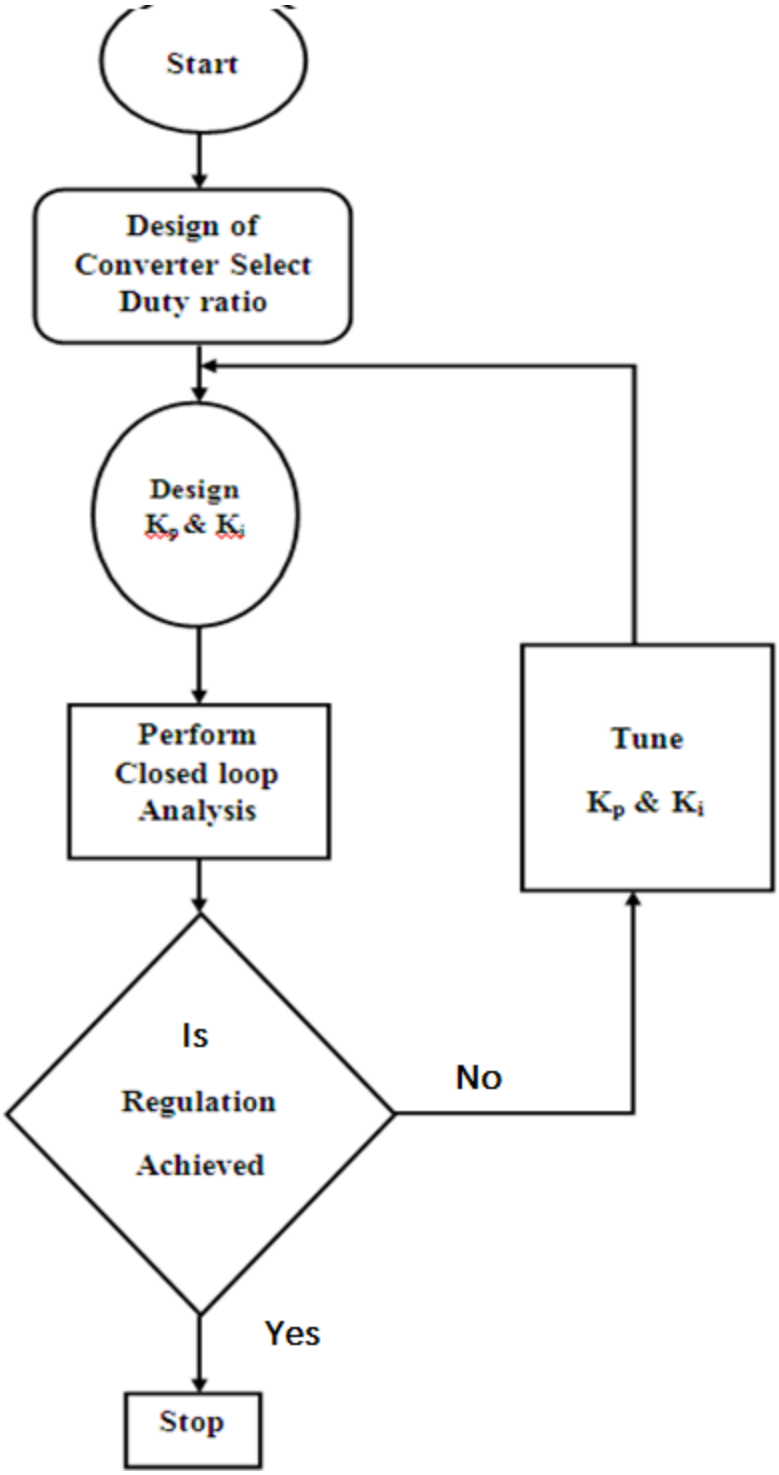

Fig.4.5.2 Flow chart for PI controlled ESEV system

The Motor speed is shown in Fig 4.6 and its value is 1180 RPM. The Motor speed (expanded speed waveform) is shown in Fig 4.7 and its value is 1150 RPM. The Torque Response is shown in Fig 4.8 and its value is 5 N-m.

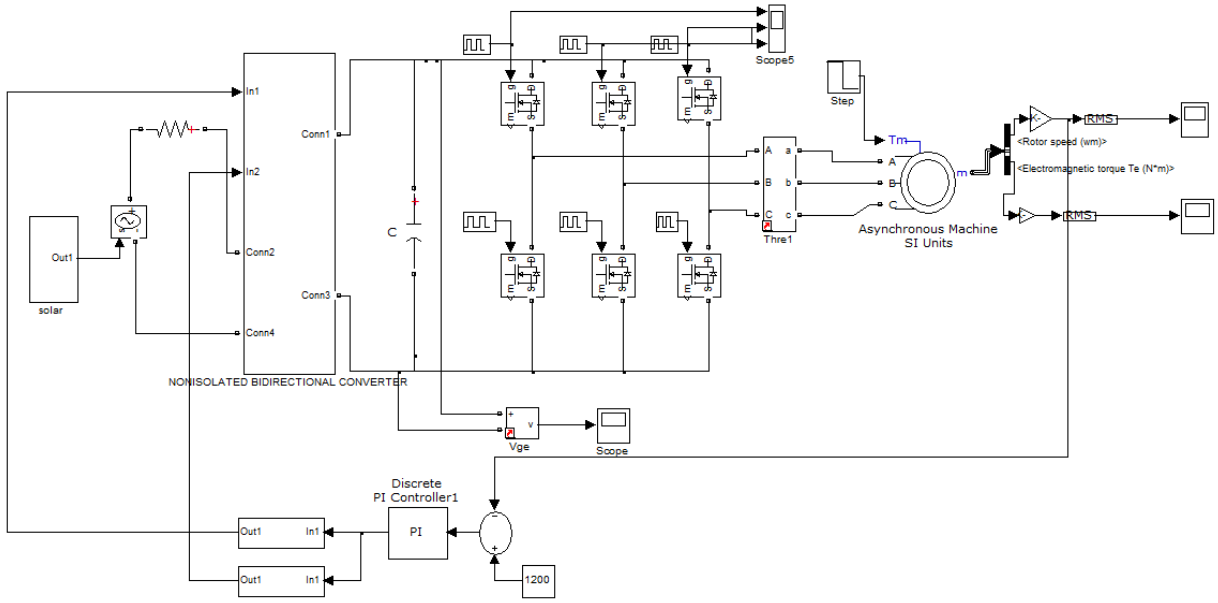

Fig 4.5 Circuit diagram of the closed-loop ESEV system with PI controller

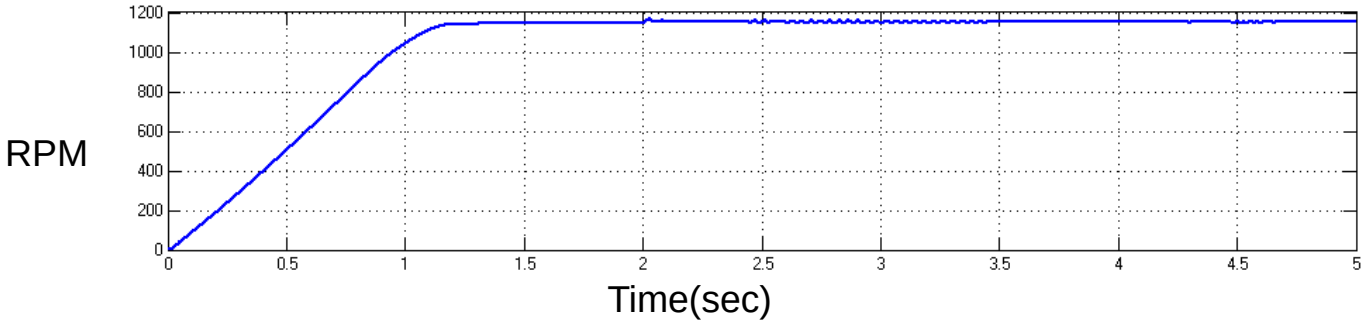

Fig 4.6 Motor speed

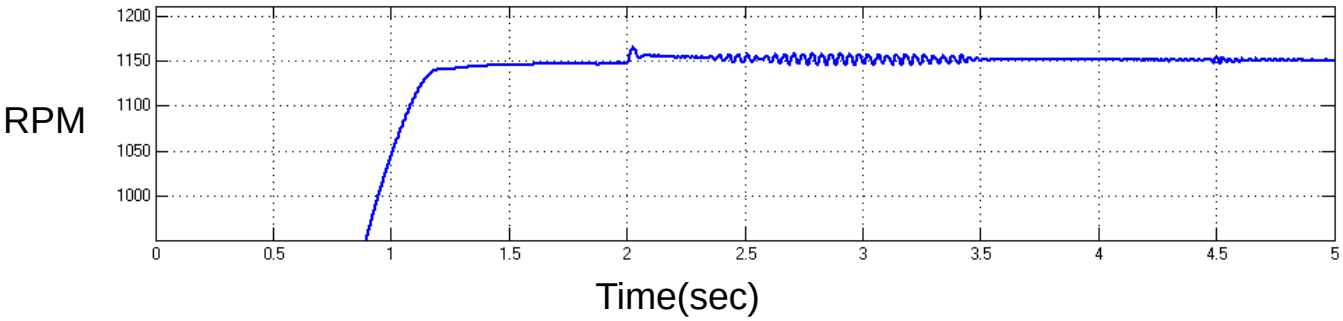

Fig 4.7 Motor speed (expanded speed waveform)

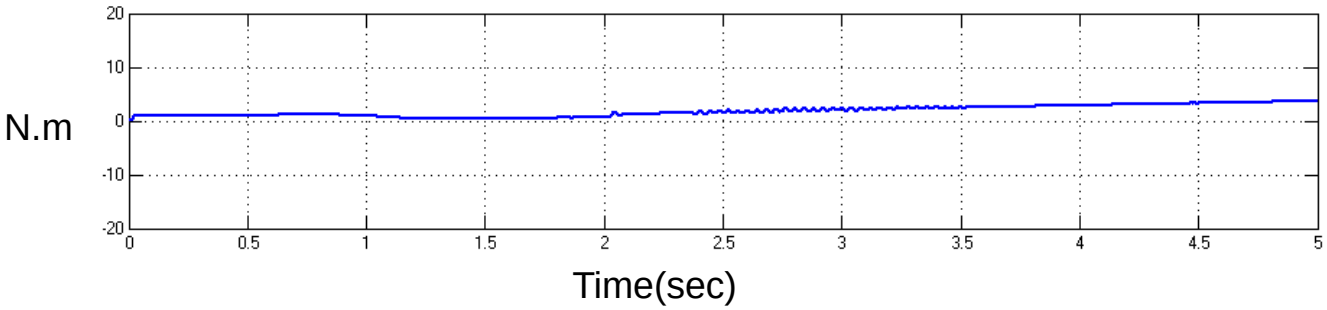

Fig 4.8 Torque Response

4.2.2 Closed-loop ESEV system with FOPID controller

The Block Diagram of FOPID controlled IMD system is shown in Fig.4.5.1. The flow chart for FOPID controlled IMD system is shown in Fig.4.5.2.

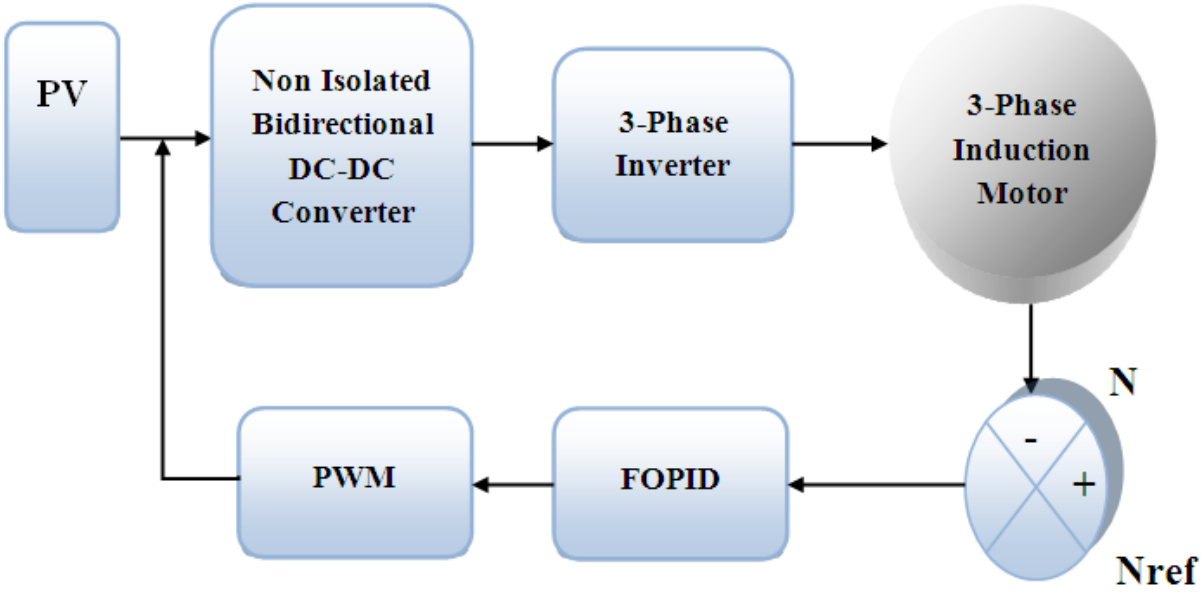

Fig 4.9.1 Closed loop ESEV system with FOPID converter

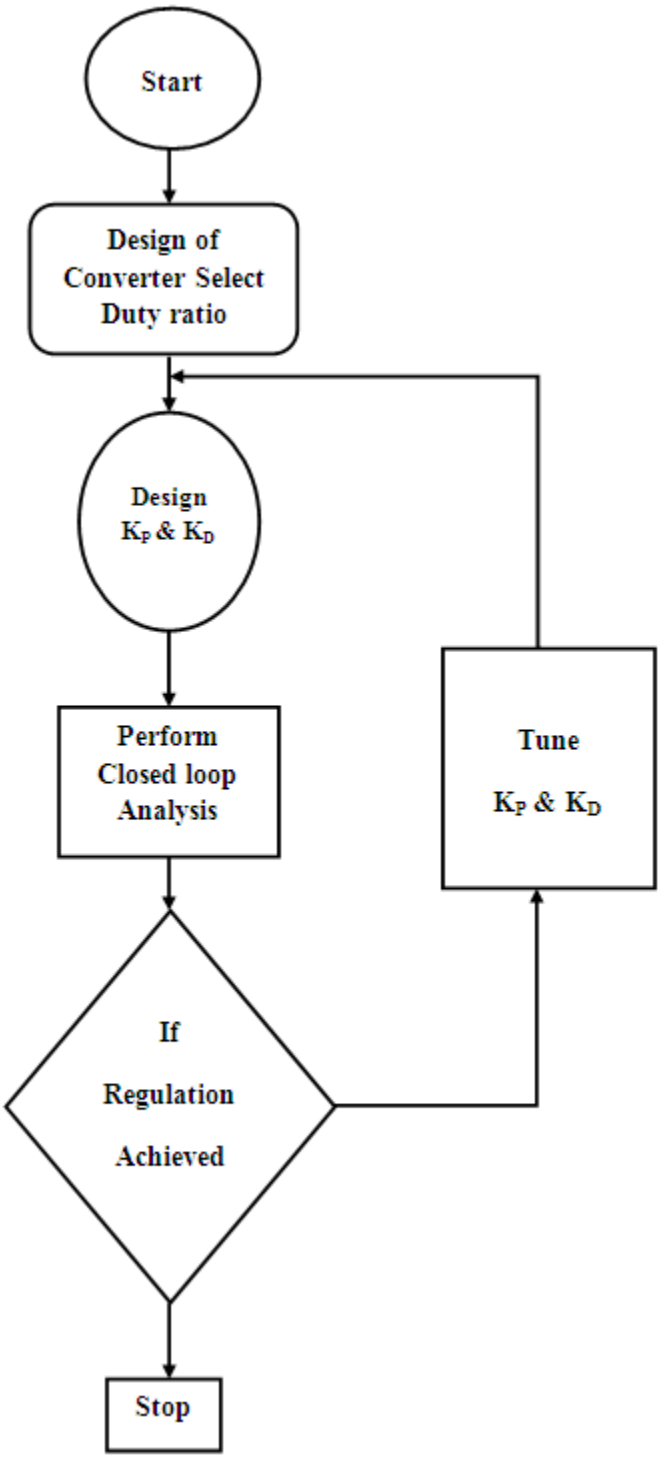

Fig 4.9.2 Flow chart of Closed loop ESEV system with FOPID converter

The circuit diagram of the closed-loop system with FOPID controller is shown in Fig 4.9. The Motor speed is shown in Fig 4.10 and its value is 1190 RPM. The Motor speed (expanded speed waveform) is shown in Fig 4.11 and the speed reduces to 1150 RPM. The Torque Response is shown in Fig 4.12 and its value is 4 N-m.

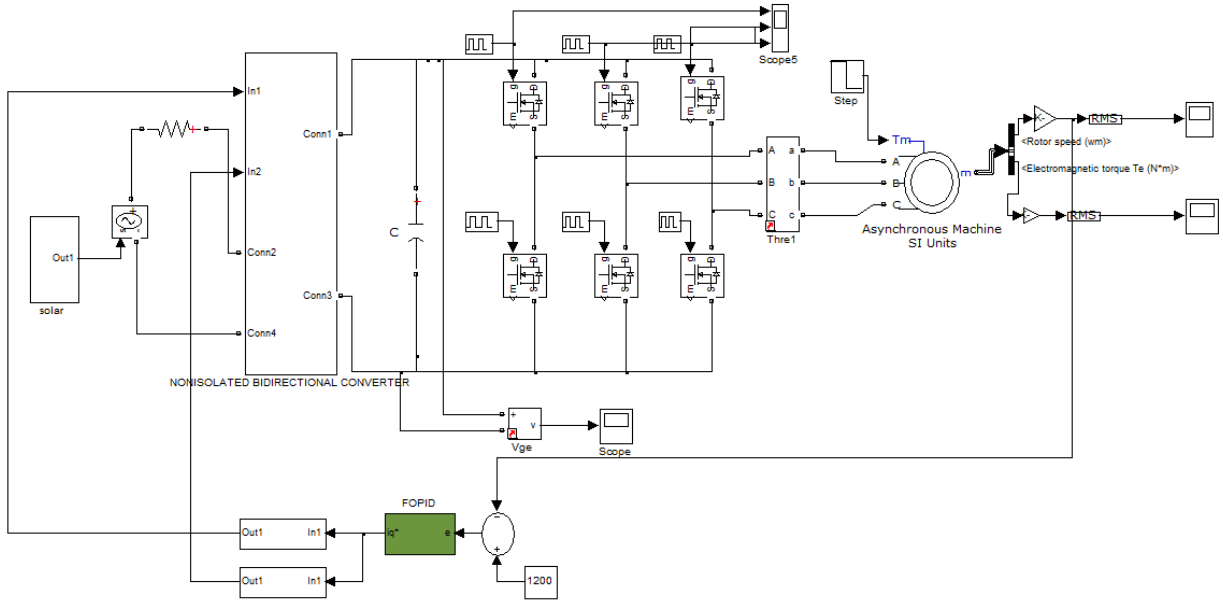

Fig 4.9 Circuit diagram of the closed-loop ESEV system with FOPID controller

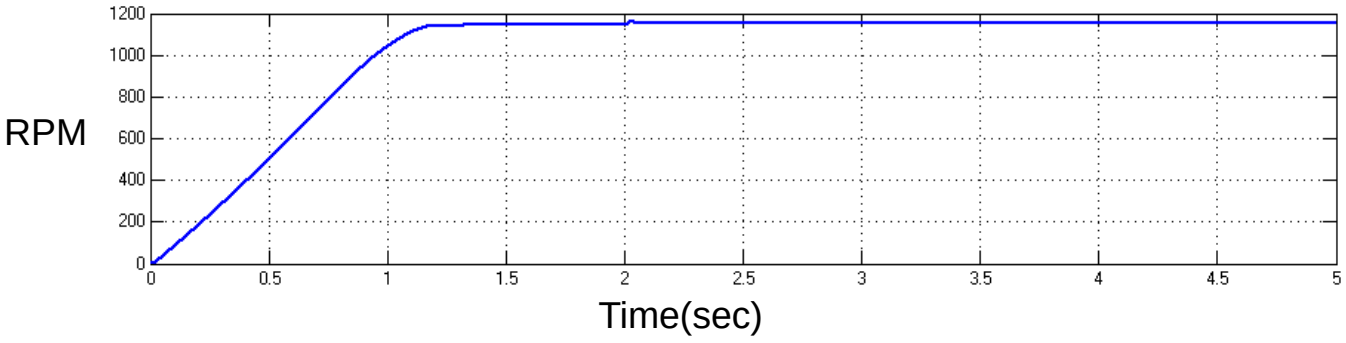

Fig 4.10 Motor speed

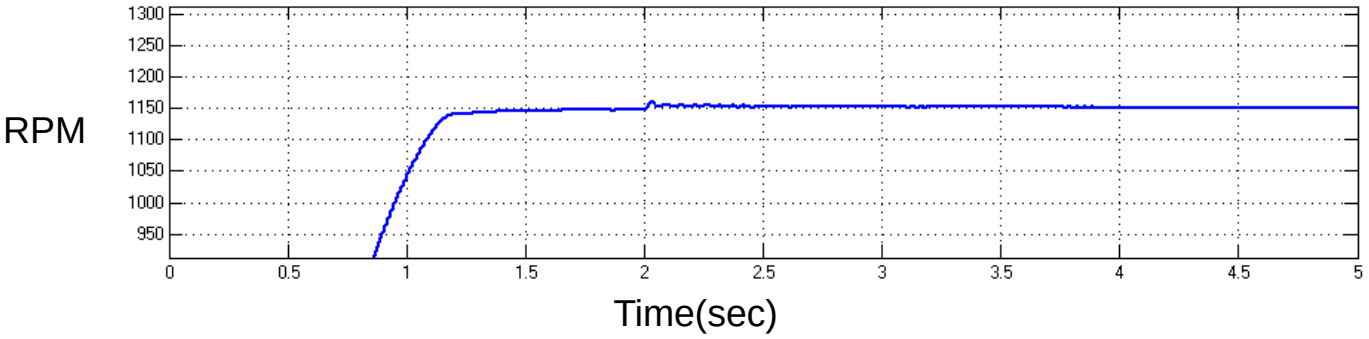

Fig 4.11 Motor speed (expanded speed waveform)

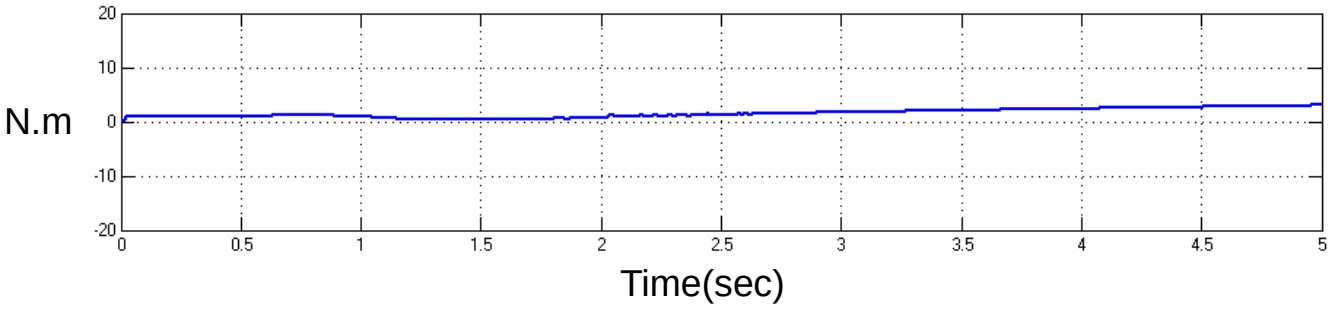

Fig 4.12 Torque Response

4.2.3 Closed-loop ESEV system with FLC controller

The Block Diagram of FL controlled IMD system is shown in Fig.4.13.1. The flow chart for FL controlled IMD system is shown in Fig.4.13.2. The control variables like error and change in error act as the input to the FLC. Using appropriate membership function,those quantities are converted into fuzzy variables(Fuzzification). Heuristic IF-THEN rules are used to define the control strategy.The control signal is again converted into the pulses (Defuzzification), which is used to trigger the switches. The available heuristic expert knowledge about the system operation is used in the fuzzification,rule base, and defuzzification stages. The fuzzy method used here is Mamdani, where the maximum of minimum composition technique is used for the inference.

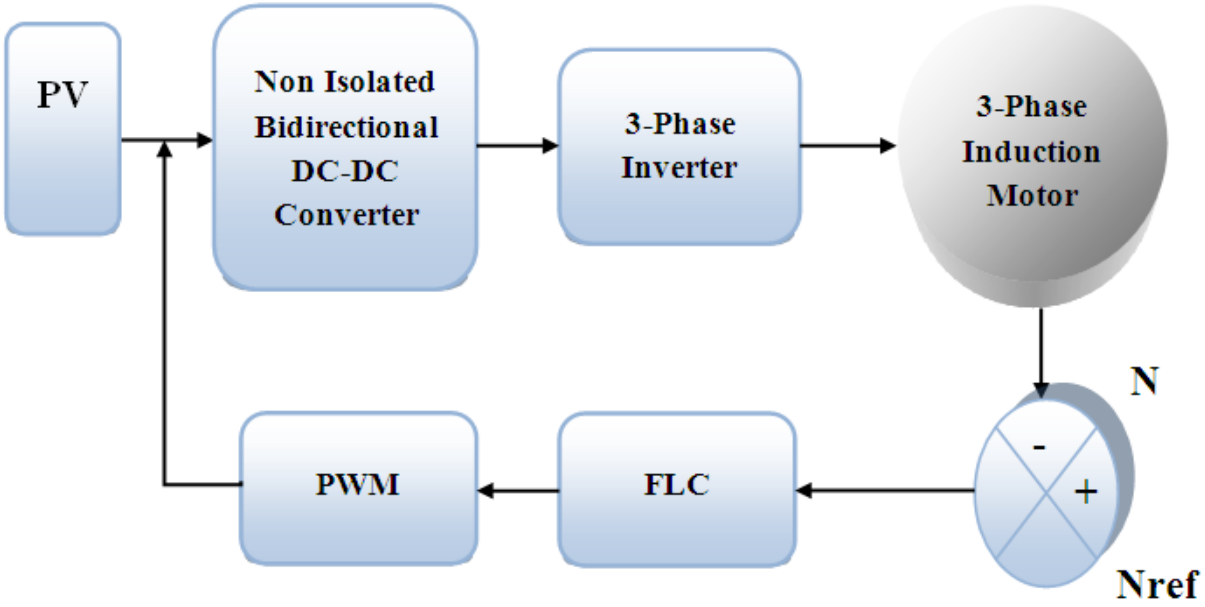

Fig 4.13.1 Closed loop ESEV system with FLC converter

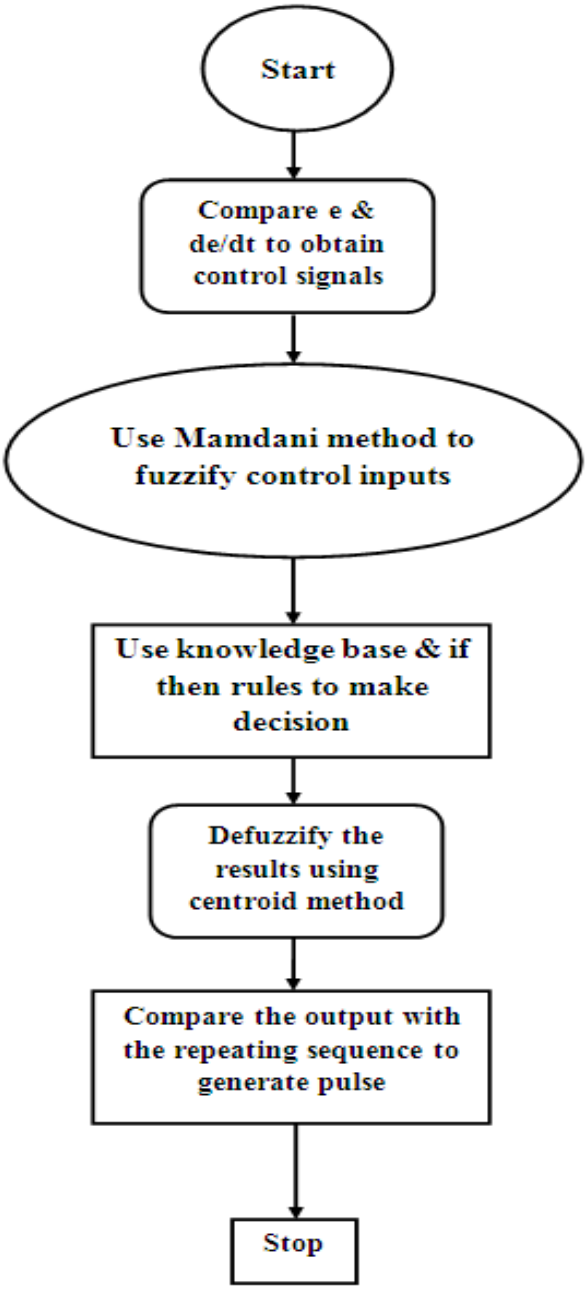

Fig 4.13.2.Flow chart for FL controlled ESEV system

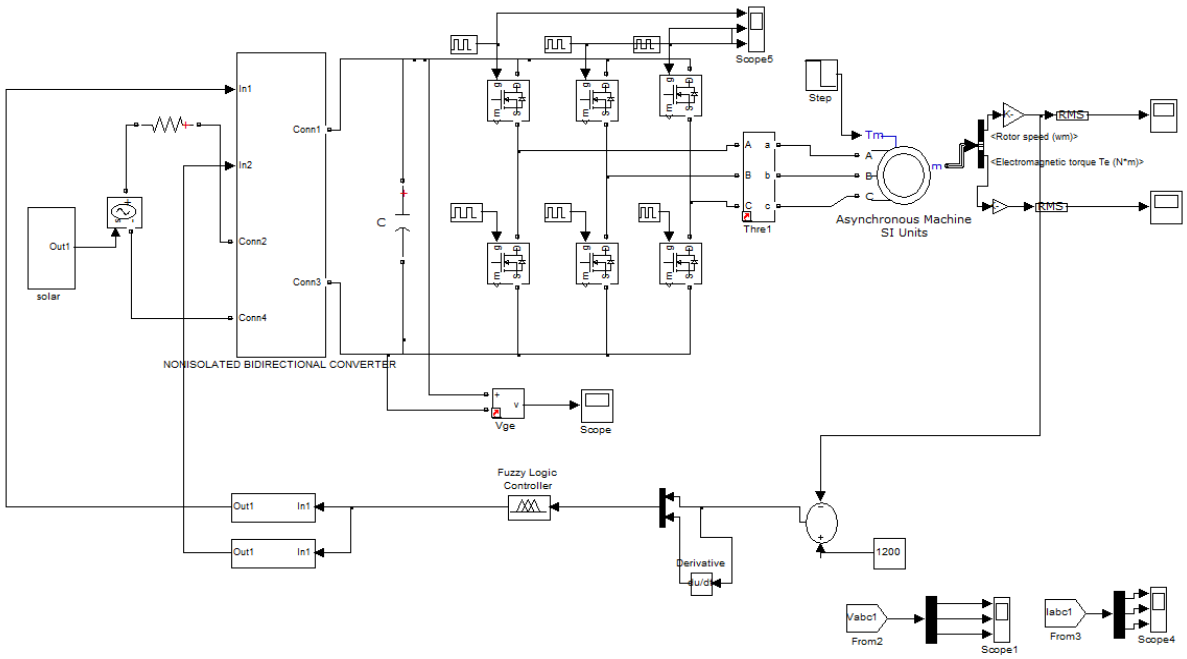

Fig 4.13.3 Circuit diagram of the closed-loop ESEV system with FLC controller

The circuit diagram of the closed-loop system with FLC is shown in Fig 4.13.3. The Motor speed is shown in Fig 4.14 and its value is 1200 RPM. The Motor speed (expanded speed waveform) is shown in Fig 4.15 and its value is 1150 RPM. The Torque Response is shown in Fig 4.16 and its value is 3 N-m. The Comparison of Time domain parameters are given in Table-3.2.It can be seen that the response with FLC is faster than that of FOPID and PI controlled systems.

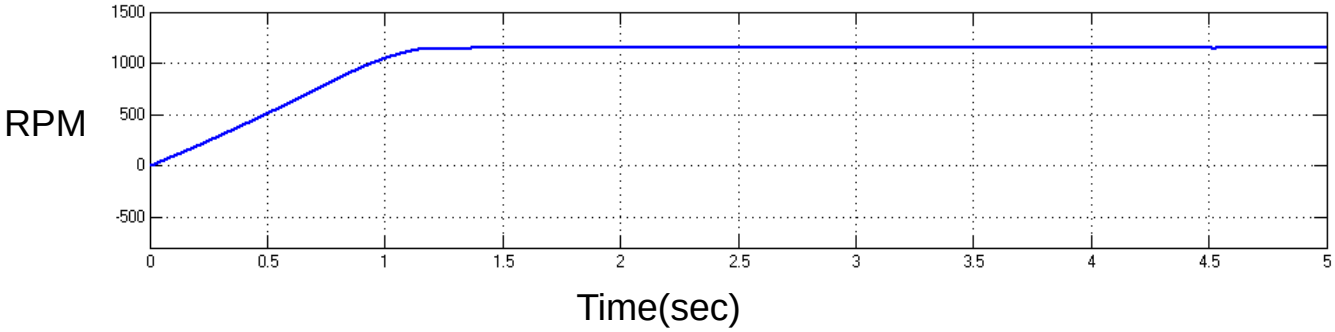

Fig 4.14 Motor speed

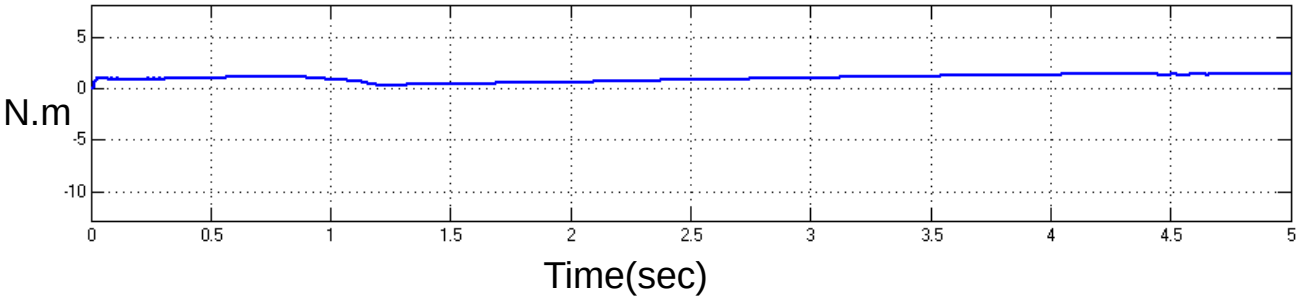

Fig 4.15 Torque Response

Table-3.2

Comparison of Time domain parameters

Controller	Tr	Ts	Tp	Ess
PI	**2.2**	**3.5**	**2.1**	**2.3**
FOPID	**2.1**	**2.5**	**2.05**	**1.7**
FLC	**0.9**	**1.2**	**1.1**	**0.9**

4.3Chapter Summary

The Open-loop ESEV system with an increase in load is simulated. The Closed-loop PI controlled ESEV system with an increase in load is simulated. The Closed-loop FOPID and FL controlled ESEV systems with an increase in load are simulated.

CHAPTER 5

CLOSED LOOP SYSTEM WITH CHANGE IN INPUT VOLTAGE

5.1 General

This chapter deals with simulation results of closed loop system with change in input voltage

Simulation Results

5.1.1Open-loop system with increase in voltage

The circuit diagram of the open-loop system with disturbance is shown in Fig 5.2. The input voltage is shown in Fig 5.3 and its value is 75 V. The Motor speed is shown in Fig 5.4 and its value is 1200 RPM. The Torque Response is shown in Fig 5.5 and its value is 0.25 N-m.

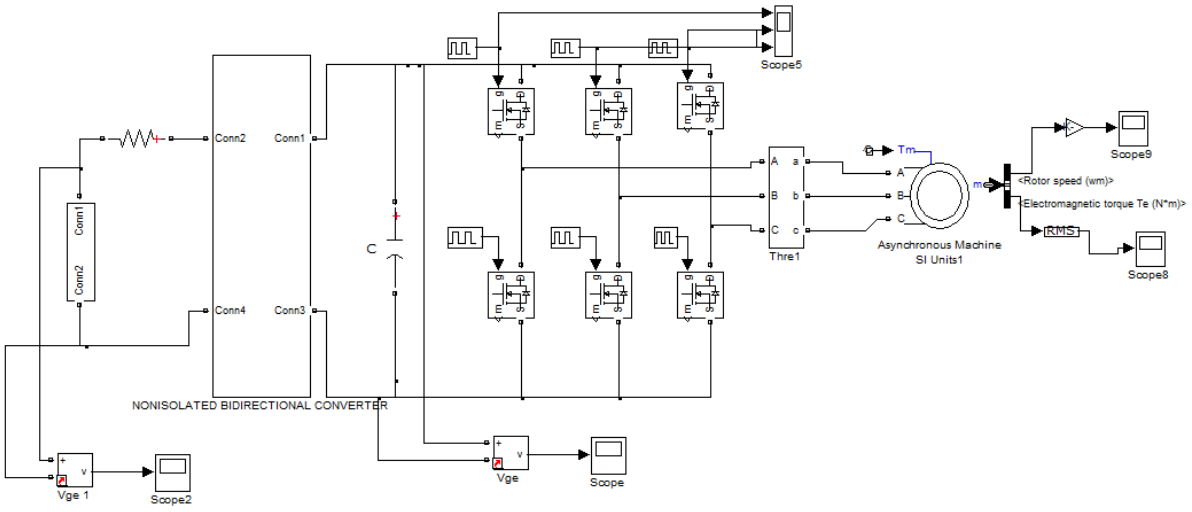

Fig 5.2 Circuit diagram of the open-loop system with increase in voltage

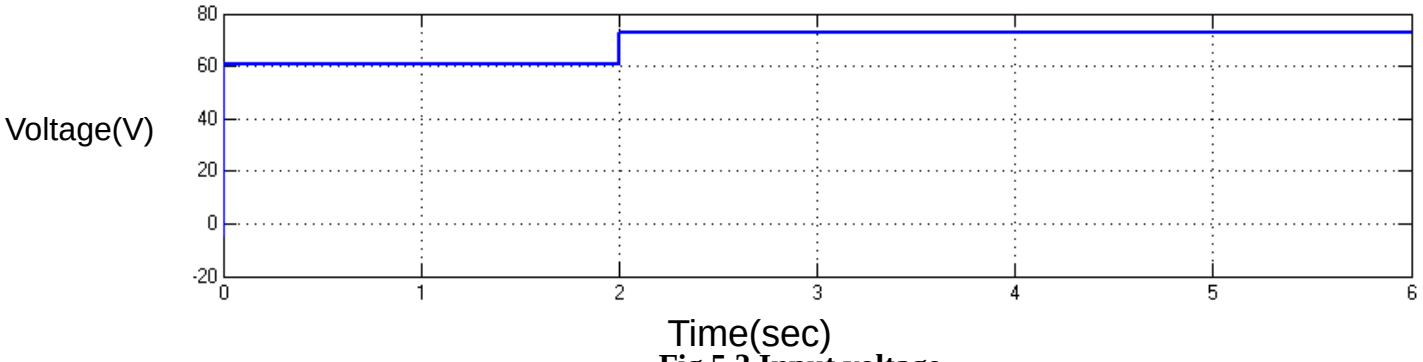

Fig 5.3 Input voltage

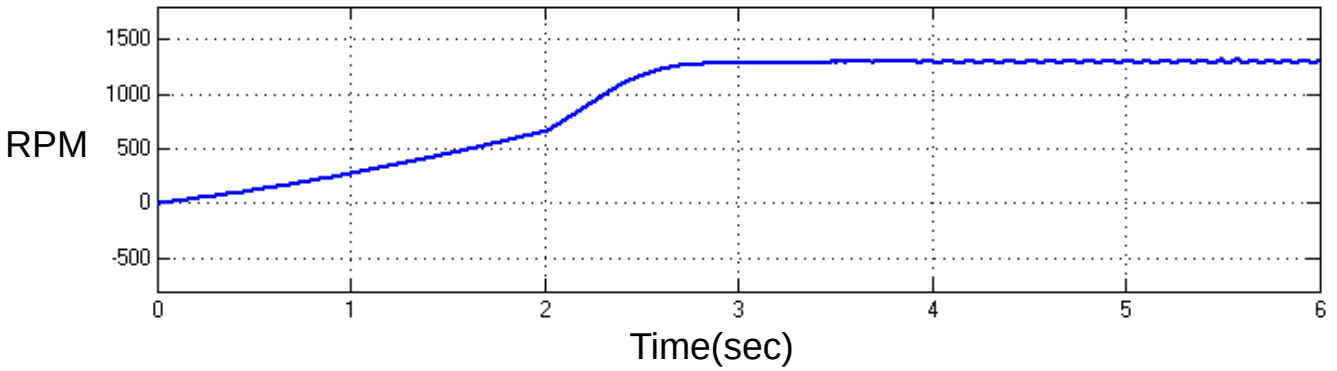

Fig 5.4 Motor speed

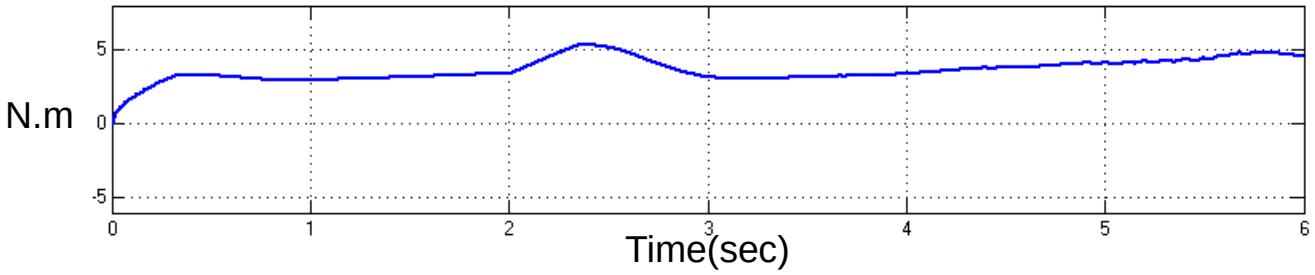

Fig 5.5 Torque Response

5.1.2 Closed-loop system with PI controller for increase in input voltage

The circuit diagram of the closed-loop system with PI controller is shown in Fig 5.6. The input voltage is shown in Fig 5.7 and its value is 75 V. The Motor speed is shown in Fig 5.8 and its value is 1200 RPM. The Torque Response is shown in Fig 5.9 and its value is 0.25 N-m.

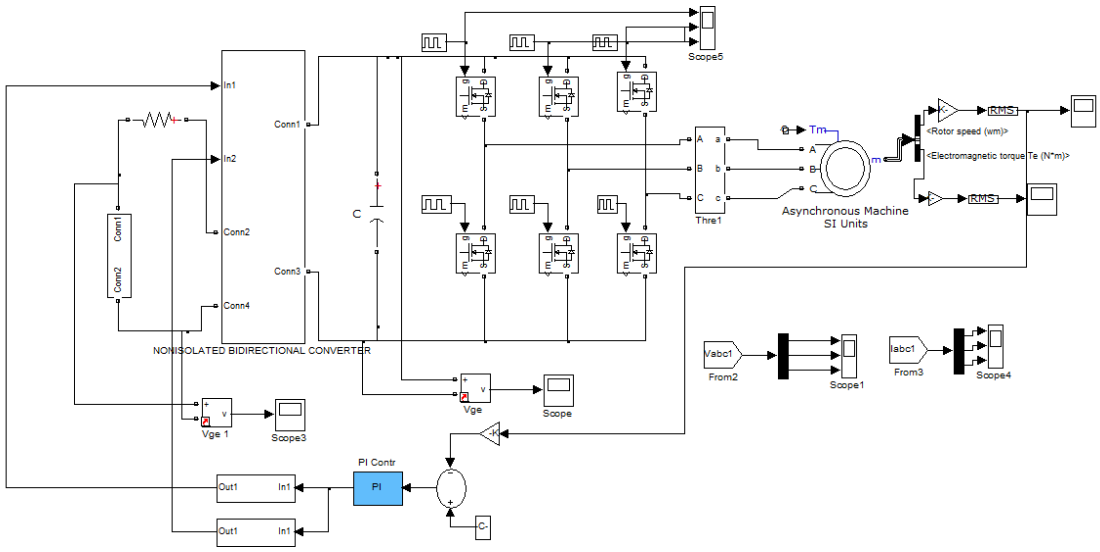

Fig 5.6 Circuit diagram of the closed-loop system with PI controller

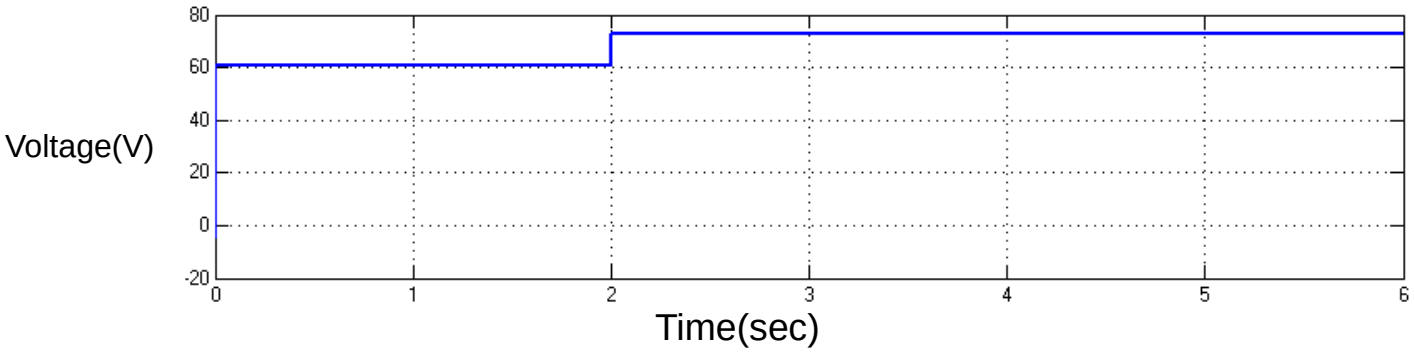

Fig 5.7 Input voltage

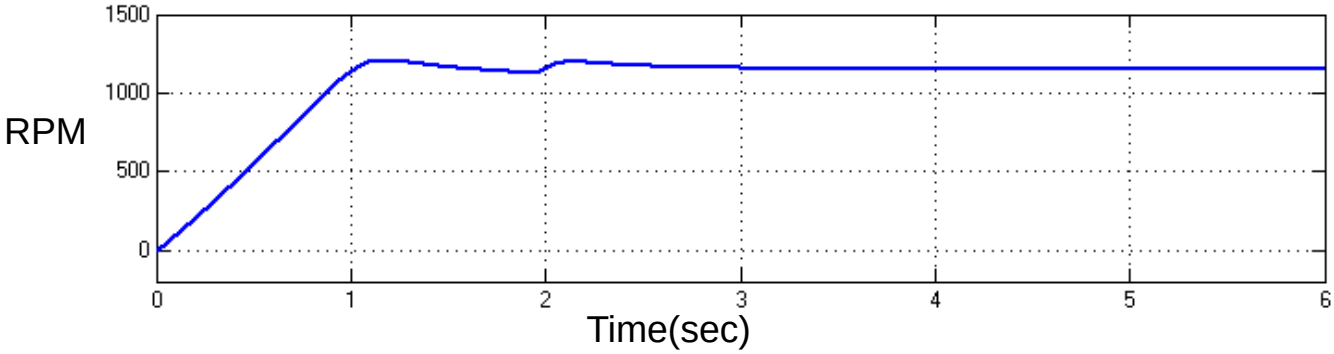

Fig 5.8 Motor speed

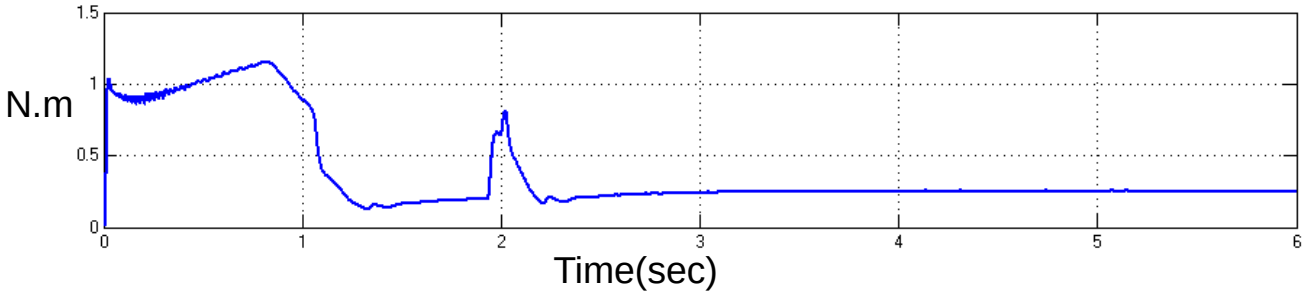

Fig 5.9 Torque Response

5.1.3 Closed-loop system with FOPID controller for increase in input voltage

Block diagram for FOPID controlled ESEV system is shown in Fig 5.10.1.The flow chart for FOPID controlled ESEV system is shown in Fig.5.10.2.

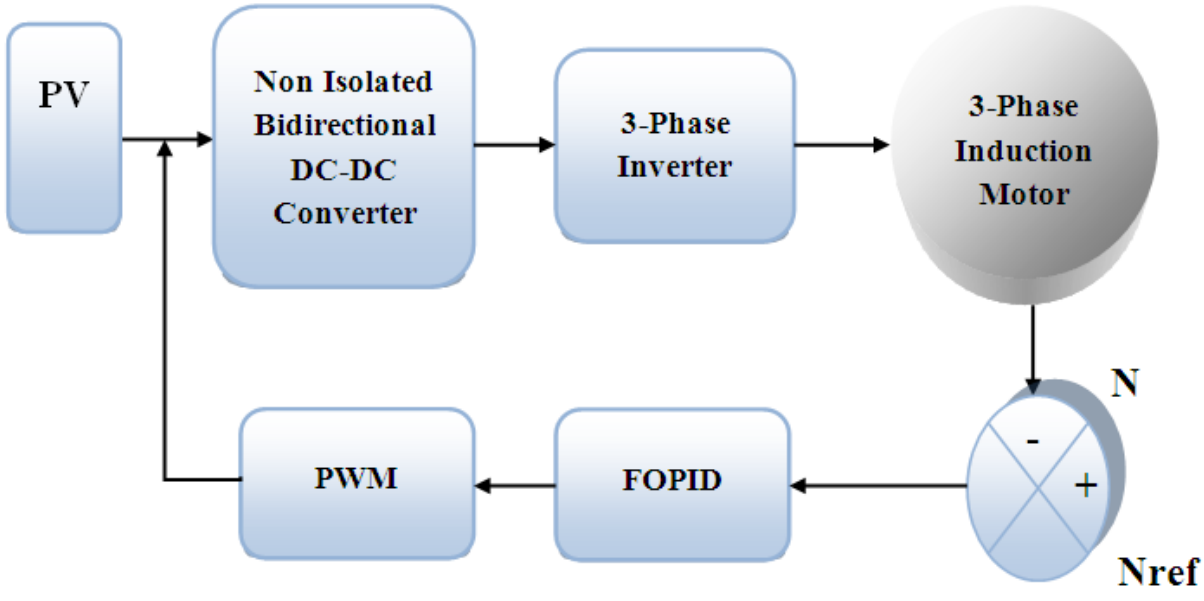

Fig 5.10.1 Block diagram for FOPID controlled ESEV system

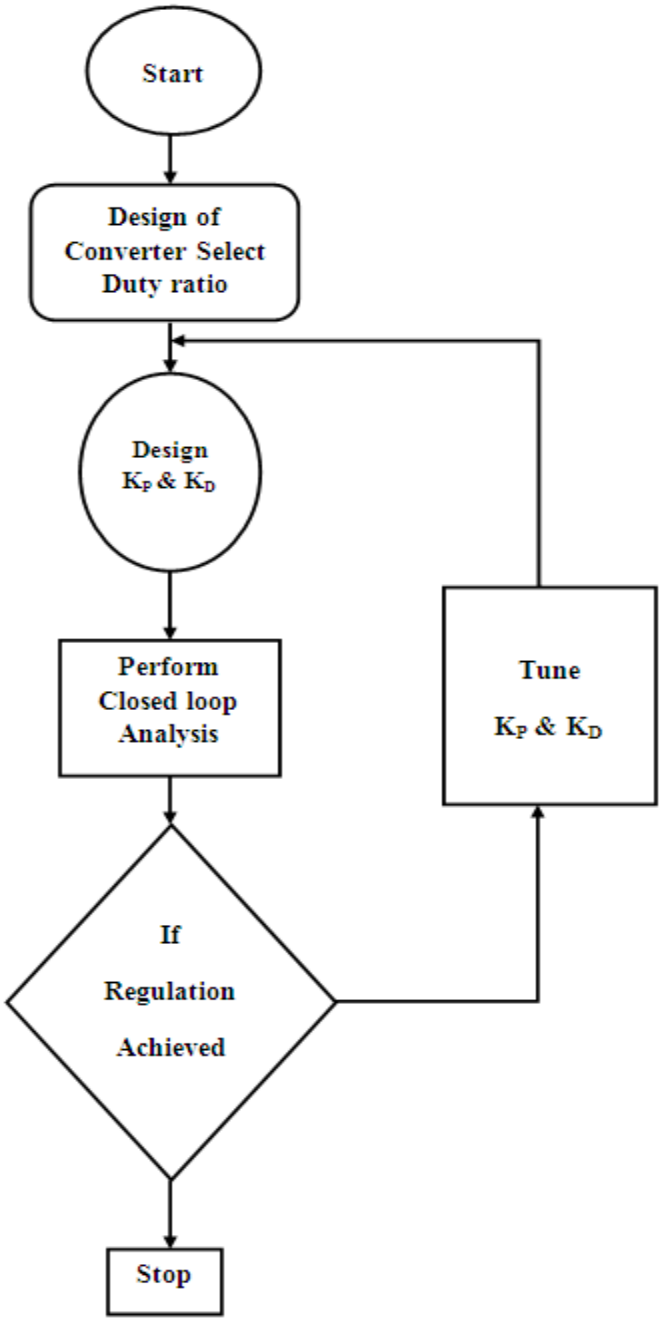

Fig 5.10.2. Flow chart for FOPID controlled ESEV system

The circuit diagram of the closed-loop system with FOPID controller is shown in Fig 5.10. 3.The input voltage is shown in Fig 5.11 and its value is 75 V. The Motor speed is shown in Fig 5.12 and its value is 1250 RPM. The Motor speed (expanded speed waveform) is shown in Fig 5.13 . The Torque Response is shown in Fig 5.14 and its value is 2.5 N-m. The Comparison of Time domain parameters are given in Table-5.1. The results indicate that the settling time is reduced from 2.4 to 2.2 seconds and the steady-state error is reduced from 2.3 V to 1.6 V using a FOPID controller.

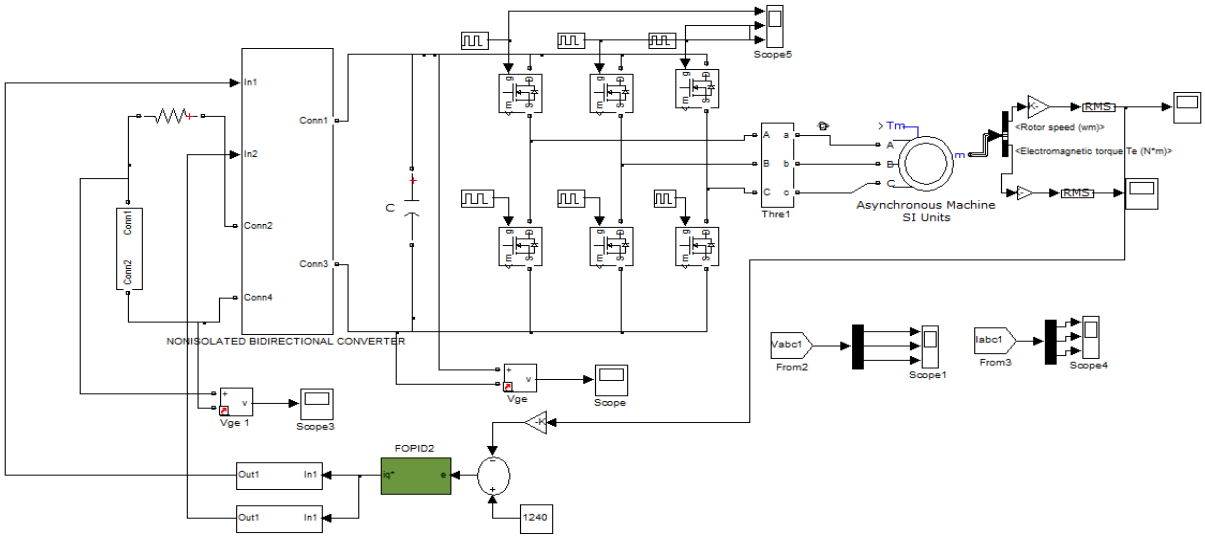

Fig 5.10.3 Circuit diagram of the closed loop system with FOPID controller

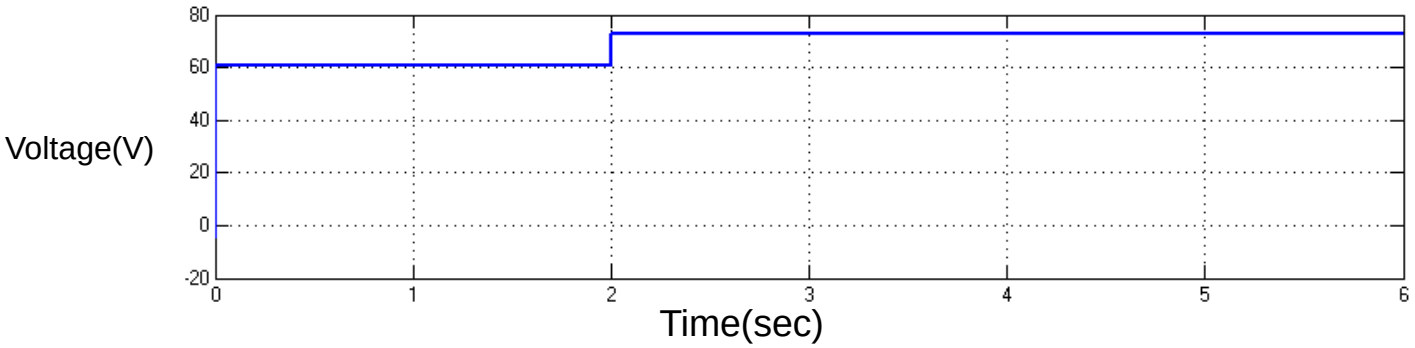

Fig 5.11 Input voltage

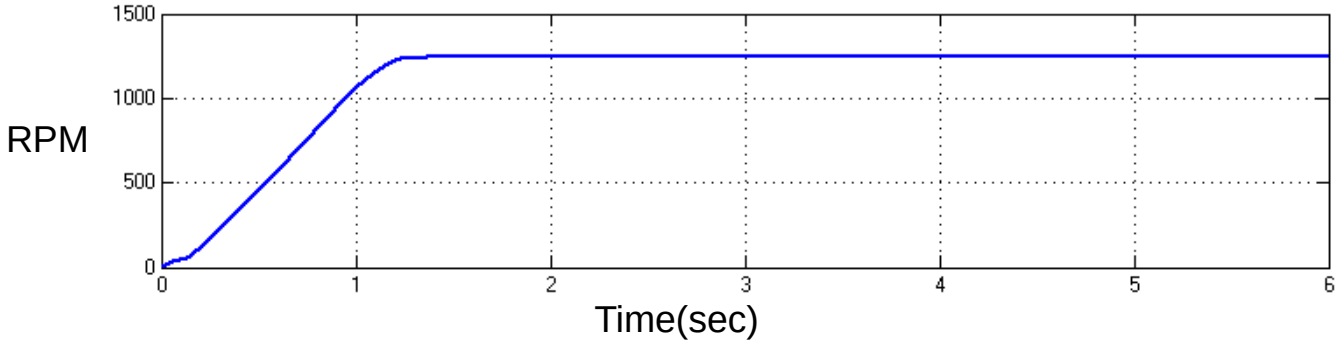

Fig 5.12 Motor speed

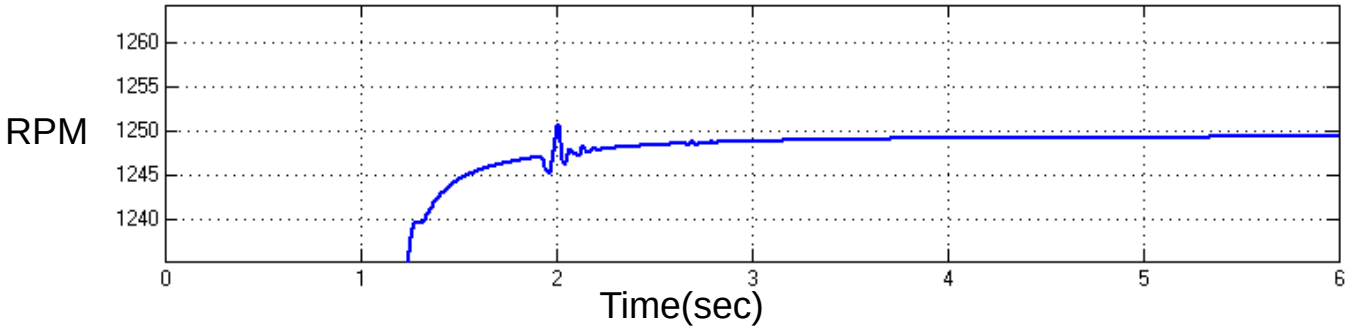

Fig 5.13 Motor speed (expanded speed waveform)

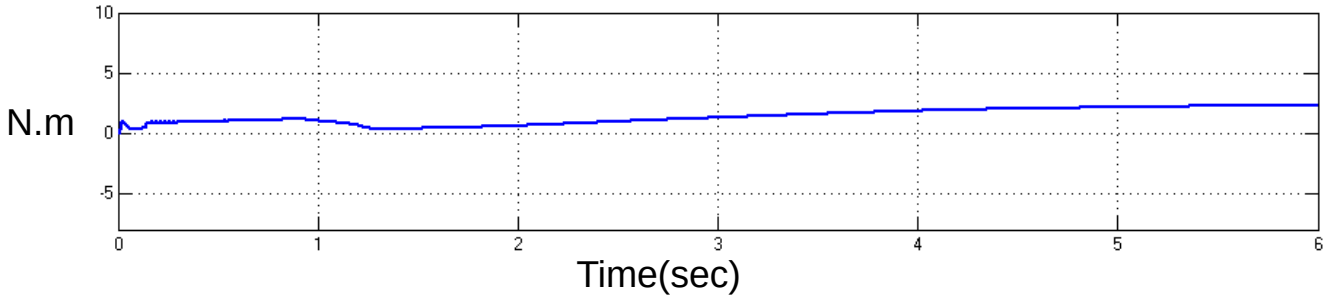

Fig 5.14 Torque Response

Table-5.1 Comparison of Time domain parameters

Controller	Tr	Ts	Tp	Ess
PI	2.2	2.7	2.4	2.3
FOPID	2.1	2.3	2.2	1.6

5.3 Chapter Summary

The open-loop ESEV system with an increase in voltage is simulated. The closed-loop PI controlled ESEV system with an increase in voltage is simulated. The closed-loop PI and FOPID controlled ESEV systems with an increase in voltage are simulated.

CHAPTER 6

CONCLUSION

The ESEV system is modeled and simulated. The results of the PI controller based Boost-converter fed ESEV system is compared with those of the FOPID-controlled inverter system. The bi-directional DC-AC system can operate in a forward mode as well as a reverse mode.

By replacing the PI controller with a FOPID controller, the settling time is reduced from 3.5secs to 2.5secs. Also, the Steady-state error in speed is reduced from 2.3secs to 1.7secs. Therefore, the response with FOPID controller is faster than the PI controlled system. Therefore FOPID controlled ESEV system is superior to the PI-controlled ESEV system. The results of time response indicates that FL based ESEV system has best dynamic response. The ESEV system has various advantages like low maintenance cost and improved time response. The disadvantage of the ESEV system is that it requires two sources.

The scope of the present work is to compare PI-controlled ESEV system with FOPID and FL controlled ESEV systems. The comparison between PI and PR controlled ESEV systems will be focused in the future.

REFERENCES

[1]. P. Y. Kong and G. K. Karagiannidis, \Charging schemes for plug-in hybrid electric vehicles in smart grid: A survey," IEEE Access, vol. 4, pp. 6846{6875, 2016.

[2]. C. for Biological Diversity. Transportation and global warming. [On- line]. Available: http://www.biologicaldiversity.org/programs/climate-law-institute/ transportation-and-global-warming

[3]. EPA, \Inventory of us greenhouse gas emissions and sinks: 1990-2009," Environmental Protection Agency2012, 2011.

[4]. N. R. Council et al., Transitions to Alternative Transportation Technologies^a:" Plug-in Hybrid Electric Vehicles. National Academies Press, 2010.

[5]. G. Lacey, G. Putrus, and E. Bentley, \Smart ev charging schedules: supporting the grid and protecting battery life," IET Electrical Systems in Transportation, vol. 7, no. 1, pp. 84{91, 2017.

[6]. B. Wang, Y. Wang, H. Nazaripouya, C. Qiu, C. C. Chu, and R. Gadh, \Predictive schedul- ing framework for electric vehicles with uncertainties of user behaviors," IEEE Internet of Things Journal, vol. 4, no. 1, pp. 52{63, Feb 2017.

[7]. Z. Fan, P. Kulkarni, S. Gormus, C. Efthymiou, G. Kalogridis, M. Sooriyabandara, Z. Zhu, S. Lambotharan, and W. H. Chin, \Smart grid communications: Overview of research challenges, solutions, and standardization activities," IEEE Communications Surveys & Tutorials, vol. 15, no. 1, pp. 21{38, 2013. 21

[8]. E. Sortomme and M. A. El-Sharkawi, \Optimal charging strategies for unidirectional vehicle-to-grid," IEEE Transactions on Smart Grid, vol. 2, no. 1, pp. 131{138, 2011.

[9]. M. T. R. Kevin Bullis. Could electric cars threaten the grid? [Online]. Available: https://www.technologyreview.com/s/518066/could-electric-cars-threaten-the-grid/

[10]. L. Yang, J. Zhang, and H. V. Poor, \Risk-aware day-ahead scheduling and real-time dis- patch for electric vehicle charging," IEEE Transactions on Smart Grid, vol. 5, no. 2, pp. 693{702, March 2014. [

[11]. M. Esmaili and M. Rajabi, \Optimal charging of plug-in electric vehicles observing power grid constraints," IET Generation, Transmission & Distribution, vol. 8, no. 4, pp. 583{590, 2014.

[12]. J. A. P. Lopes, F. J. Soares, and P. M. R. Almeida, \Integration of electric vehicles in the electric power system," Proceedings of the IEEE, vol. 99, no. 1, pp. 168{183, 2011.

[13]. O. Sundstrom and C. Binding, \Flexible charging optimization for electric vehicles consid- ering distribution grid constraints," IEEE Transactions on Smart Grid, vol. 3, no. 1, pp. 26{37, 2012.

[14]. N. Rotering and M. Ilic, \Optimal charge control of plug-in hybrid electric vehicles in deregulated electricity markets," IEEE Transactions on Power Systems, vol. 26, no. 3, pp. 1021{1029, 2011.

[15]. S. G. Yoon, Y. J. Choi, J. K. Park, and S. Bahk, \Stackelberg-game-based demand response for at-home electric vehicle charging," IEEE Transactions on Vehicular Technology, vol. 65, no. 6, pp. 4172{4184, June 2016.

[16]. S. Maharjan, Q. Zhu, Y. Zhang, S. Gjessing, and T. Basar, \Dependable demand response management in the smart grid: A stackelberg game

approach," IEEE Transactions on Smart Grid, vol. 4, no. 1, pp. 120{132, 2013.

[17]. A. Zakariazadeh, S. Jadid, and P. Siano, \Smart microgrid energy and reserve scheduling with demand response using stochastic optimization," International Journal of Electrical Power & Energy Systems, vol. 63, pp. 523{533, 2014. 22

[18]. M. C. Falvo, G. Graditi, and P. Siano, \Electric vehicles integration in demand response programs," in Power Electronics, Electrical Drives, Automation and Motion (SPEEDAM), 2014 International Symposium on, June 2014, pp. 548{553.

[19]. M. Yu and S. H. Hong, \A real-time demand-response algorithm for smart grids: A stack- elberg game approach," IEEE Transactions on Smart Grid, vol. 7, no. 2, pp. 879{888, 2016.

[20]. A.-H. Mohsenian-Rad, V. W. Wong, J. Jatskevich, R. Schober, and A. Leon-Garcia, \Au- tonomous demand-side management based on game-theoretic energy consumption schedul- ing for the future smart grid," IEEE transactions on Smart Grid, vol. 1, no. 3, pp. 320{331, 2010.

[21]. Z. Fan, \Distributed demand response and user adaptation in smart grids," in Integrated Network Management (IM), 2011 IFIP/IEEE International Symposium on. IEEE, 2011, pp. 726{729.

[22]. A. J. Conejo, J. M. Morales, and L. Baringo, \Real-time demand response model," IEEE Transactions on Smart Grid, vol. 1, no. 3, pp. 236{242, 2010.

[23]. C. Wang and M. De Groot, \Managing end-user preferences in the smart grid," in Proceed- ings of the 1st International Conference on Energy-E

[24]. S. Caron and G. Kesidis, \Incentive-based energy consumption scheduling algorithms for the smart grid," in Smart grid communications

(SmartGridComm), 2010 First IEEE in- ternational conference on. IEEE, 2010, pp. 391{396.

[25]. Y. Tang, J. Zhong, and M. Bollen, \Aggregated optimal charging and vehicle-to-grid control for electric vehicles under large electric vehicle population," IET Generation, Transmission & Distribution, vol. 10, no. 8, pp. 2012{2018, 2016.

[26]. A. H. Mohsenian-Rad, V. W. S.Wong, J. Jatskevich, R. Schober, and A. Leon-Garcia, \Au- tonomous demand-side management based on game-theoretic energy consumption schedul- ing for the future smart grid," IEEE Transactions on Smart Grid, vol. 1, no. 3, pp. 320{331, Dec 2010. 23

[27]. P. Yang, G. Tang, and A. Nehorai, \A game-theoretic approach for optimal time-of-use electricity pricing," IEEE Transactions on Power Systems, vol. 28, no. 2, pp. 884{892, 2013.

[28]. Z. Ma, D. S. Callaway, and I. A. Hiskens, \Decentralized charging control of large pop- ulations of plug-in electric vehicles," IEEE Transactions on Control Systems Technology, vol. 21, no. 1, pp. 67{78, Jan 2013.

[29]. W. Tushar, W. Saad, H. V. Poor, and D. B. Smith, \Economics of electric vehicle charging: A game theoretic approach," IEEE Transactions on Smart Grid, vol. 3, no. 4, pp. 1767{ 1778, 2012.

[30]. T. Basar and G. J. Olsder, \Dynamic noncooperative game theory (classics in applied mathematics)," 1999.

[31]. F. P. Kelly, A. K. Maulloo, and D. K. Tan, \Rate control for communication networks: shadow prices, proportional fairness and stability," Journal of the Operational Research society, vol. 49, no. 3, pp. 237{252, 1998.

[32]. R. Srikant, \The mathematics of internet congestion control, ser. series: Systems and control: Foundations and applications," 2004.

[33]. T. Basar and R. Srikant, \Revenue-maximizing pricing and capacity expansion in a many- users regime," in INFOCOM 2002. Twenty-First Annual Joint Conference of the IEEE Computer and Communications Societies. Proceedings. IEEE, vol. 1. IEEE, 2002, pp. 294{301.

[34]. J. Kennedy and R. Eberhart, \Particle swarm optimization," in Neural Networks, 1995. Proceedings., IEEE International Conference on, vol. 4, Nov 1995, pp. 1942{1948 vol.4.